

**INDUSTRIAL FAULT DETECTION AND DIAGNOSIS USING BAYESIAN BELIEF
NETWORK**

by

© Hassan Gharahbagheri

A thesis submitted to the

School of Graduate Studies

in partial fulfillment of the requirement for the degree of

Master of Engineering

Faculty of Engineering and Applied Science

Memorial University of Newfoundland

May 2016

St. John's

Newfoundland and Labrador

Abstract

Rapid development in industry have contributed to more complex systems that are prone to failure. In applications where the presence of faults may lead to premature failure, fault detection and diagnostics tools are often implemented. The goal of this research is to improve the diagnostic ability of existing FDD methods. Kernel Principal Component Analysis has good fault detection capability, however it can only detect the fault and identify few variables that have contribution on occurrence of fault and thus not precise in diagnosing. Hence, KPCA was used to detect abnormal events and the most contributed variables were taken out for more analysis in diagnosis phase. The diagnosis phase was done in both qualitative and quantitative manner. In qualitative mode, a networked-base causality analysis method was developed to show the causal effect between the most contributing variables in occurrence of the fault. In order to have more quantitative diagnosis, a Bayesian network was constructed to analyze the problem in probabilistic perspective.

Acknowledgement

Looking back over the past two years, I can see many people who deserve credit for their contributions to this research throughout my graduate studies.

First of all, I would like to express my sincere gratefulness to my academic advisors, Dr. Khan and Dr. Imtiaz, for their ideas, inspiration, and patience, for their providing me this opportunity of studying abroad, and encouraging me all the time.

I would like to thank my family for their support and encouragement. Especially there is an eternal appreciation with love to my mother which made all this possible.

During the program, I met lots of colleagues who gave me supports in their own way, as I needed to keep going. Hence, I feel grateful to all my colleagues at the Safety and Risk Engineering Group (SREG) especially Anirudh Nandan and Ahmed Abdallah.

Certainly, I highly appreciate my family, for their endless spiritual encouragement and trust, which support me to accomplish this dissertation.

I would also like to gratefully acknowledge the financial support provided by Natural Sciences and Engineering Research Council (NSERC).

Table of content

Abstract.....	i
Acknowledgement.....	ii
List of tables.....	vii
List of figures.....	ix
List of symbols, nomenclature or abbreviations.....	xii
Chapter 1: Introduction	
1.1. Background	1
1.2. Objective.....	2
1.3. Thesis structure.....	3
Chapter 2: Literature review	
2.1. Background.....	4
2.2. Fault detection and diagnosing the root cause of the fault.....	5
2.2.1. Model-based fault detection and diagnosis.....	6
2.2.2. Process history-based FDD.....	8
2.2.3. Knowledge based methods inn FDD.....	12
2.2.3.1. Fault tree analysis.....	12
2.2.3.2. Signed digraph.....	13

2.2.3.3. The possible cause and effect graph.....	13
2.2.3.4. Bayesian network.....	13
2.3. Combined framework of fault detection and diagnosis.....	16
 Chapter 3: Combination and KPCA and causality analysis for root cause diagnosis of industrial process fault	
3.1. Introduction	20
3.2. Methods and techniques.....	22
3.2.1. Kernel principal component analysis.....	26
3.2.2. Causality analysis based on Granger causality.....	27
3.2.3. Causality analysis based on transfer entropy.....	29
3.2.4. Mathematical example on causality analysis.....	31
3.2.4.1. Validation by Granger causality.....	31
3.2.4.2. Validation by transfer entropy.....	32
3.3. Industrial case study.....	34
3.3.1. Fluid catalytic cracking unit.....	34
3.3.2. Tennessee Eastman Chemical Process.....	46
3.4. Conclusion.....	56

Chapter 4: Root cause diagnosis of process fault using KPCA and Bayesian network

4.1. Introduction.....	57
4.2. Methodology: networked-based process monitoring approach	62
4.2.1. Kernel principal component Analysis (KPCA)	63
4.2.2. Sensor failure module.....	65
4.2.3. Bayesian network construction.....	68
4.2.3.1. Causality analysis based on Granger causality.....	68
4.2.3.2. Causality analysis based on transfer entropy.....	70
4.2.3.3. Estimation of conditional probabilities.....	71
4.2.3.4. Construction of BN: An illustrative example.....	73
4.2.4. Loop handling.....	78
4.3. Application of proposed methodology.....	78
4.3.1. Fluid Catalytic Cracking.....	79
4.3.2. Tennessee Eastman Chemical Process.....	86
4.4. Conclusion.....	94
Appendix.....	96

Chapter 5: Summary, conclusion and future works

5.1. Conclusions.....	101
-----------------------	-----

5.2. Suggestions and future works.....102

References104

List of Tables

Table 3.1. General consideration of process monitoring tools.....	24
Table 3.2. Granger causality test results for mathematical model.....	33
Table 3.3. Mutual transfer entropy values for mathematical model.....	33
Table 3.4. Measured variable of FCC process	35
Table 3.5.fault scenarios in FCC.....	37
Table 3.6. Granger test results of variables in FCC unit. (a) fault in ambient air temperature, (b) fault in fresh feed temperature.....	44
Table 3.7. Transfer entropy between the most effective variables in two fault scenarios (a) fault in ambient temperature (b) fault in fresh feed temperature.....	45
Table 3.8. Measured variables in TE.....	47
Table 3.9.fault scenarios in TE.....	48
Table 3.10.Granger causality test for Tennessee Eastman process. (a) IDV6, (b) IDV12.....	54
Table 3.11. Transfer entropy between the most effective variables in two faulty scenarios in Tennessee Eastman (a) IDV6, (b) IDV12.....	55
Table 4.1. The result of Granger causality analysis for dissolution tank system.....	75
Table 4.2. Mutual transfer entropy values between nodes on dissolution tank system.....	75

Table 4.3. Measured variable of FCC process.....80

Table 4.4. Fault scenarios in FCC.....80

Table 4.5. Measured variables in Tennessee Eastman.....88

Table 4.6. Fault scenarios in Tennessee Eastman Chemical Process.....89

List of Figures

Figure 2.1. Fault diagnosis method	6
Figure 2.2. Model based fault detection strategy.....	7
Figure 2.3. Normal and faulty data. a. nonlinear b. linear (after applying kernel).....	11
Figure 3.1. Causality network of (a) Fluid Catalytic Cracking process (b) Tennessee Eastman Chemical Process.....	25
Figure 3.2. Schematic illustration of the proposed FDD method.....	26
Figure 3.3. Linearization with mapping function in KPCA	27
Figure 3.4. The network of mathematical example.....	34
Figure 3.5. Schematic illustration of FCC process.....	35
Figure 3.6. KPCA results for FCC (a) T^2 Hotelling. Contribution plots for (b) fault in ambient temperature (c) fault in fresh feed temperature.....	41
Figure 3.7. Causal network of two faulty scenario in FCC (a) fault on ambient temperature (b) fault on fresh feed temperature.....	45
Figure 3.8. Schematic of Tennessee Eastman process.....	46
Figure 3.9. KPCA results for Tennessee Eastman (a) T^2 Hotelling. Contribution plots for (b) IDV(6) (c) IDV(12).....	51

Figure 3.10. Constructed networks based on proposed technique for Tennessee Eastman process. (a) IDV6, (b) IDV12.....	55
Figure 4.1. The proposed method of this research.....	61
Figure 4.2. Normal and faulty states of a sensor (a) Normal performance (b) flat line fault (c) spike fault (d) noise fault.....	67
Figure 4.3. Pseudo-code for sensor fault detection.....	67
Figure 4.4. Process flow diagram of dissolution tank system ⁴¹	74
Figure 4.5. Constructed network for dissolution tank system using Granger causality and transfer entropy.....	75
Figure 4.6. Process value and generated residuals of dissolution tank system. (a) Level (b) water flow rate	77
Figure 4.7. Loop handling in Bayesian network.....	78
Figure.4.8. Schematic illustration of FCC process.....	79
Figure 4.9. Hotelling T^2 and Contribution plots for faulty scenarios in FCC.....	82-83
Figure 4.10. (a) BN for FCC process and (b) propagation pathway in FCC process (fault in ambient air temperature).....	84
Figure 4.11. (a) BN for FCC process and (b) propagation pathway in FCC process (fault in fresh feed temperature).....	86

Figure 4.12. Schematic diagram of Tennessee Eastman process.....87

Figure 4.13. T^2 Hotelling and Contribution plots for both faulty scenarios of Tennessee Eastman process91-92

Figure 4.14. (a) BN for Tennessee Eastman and (b) propagation pathway (fault is for loss in feed A).....92

Figure 4.15. (a) BN for Tennessee Eastman and (b) propagation pathway (fault is in condenser cooling water inlet temperature).....94

List of Symbols, Nomenclature or abbreviations

FDD	Fault detection and diagnosis
BN	Bayesian network
FCC	Fluid Catalytic Cracking
TE	Transfer entropy
PCA	Principal Component Analysis
KPCA	Kernel Principal Component Analysis
SDG	Signed diagraph
PCEG	The Possible Cause and Effect Graph
FTA	Fault Tree Analysis
RBC	Reconstructed-based contribution
MLE	Maximum likelihood estimation

Chapter 1

Introduction

1.1. Background

In chemical, petrochemical, food processing, papermaking, steel, power and other process industries, there has been a continuing demand for higher quality products, lower product rejection rates, and satisfying increasingly stringent safety and environmental regulation [1]. Modern control systems become extremely complex by integrating various functions and components for sophisticated performance requirement [2, 3]. With such complexities in hardware and software, it is natural that the system may become vulnerable to faults in practice and fault diagnostic tools are the main requirements to endure the process safety and quality of products. The objectives of these tools are earlier detection of problems to take actions that mitigates the fault's impact on the system [3].

Over the years, many fault detection and diagnosis methods have been developed, each method manages to capture or model some subset of the features of the diagnostic reasoning and thus may be more suitable than other techniques for a particular class of problems [4]. As such, hybrid frameworks consisting of a collection of methods performing cooperative problem solving is proposed as an alternative to individual methods. Such a hybrid framework is an effective way of utilizing all available information and overcoming limitations of individual methods [5-7]. This

combination of different methods allows one to evaluate different kinds of knowledge in one single framework for better decision making [7].

1.2. Objective

The goal of this research is to develop a process fault detection and diagnosis tool that gives definitive answer about the root cause of a fault and helps operator to save the process. To this aim, KPCA, causality analysis, and Bayesian networked-base diagnosis methods have been used in a hybrid framework. However, there are some challenges based on previous research in this area. This research tries to propose a comprehensive methodology to address those challenges. The main objectives of this research are as follows:

- We propose to improve the root cause diagnosis of KPCA through integration with knowledge based methods, i.e. Granger causality, transfer entropy, for better diagnosing of process fault's root cause.
- Using a BN to integrate process knowledge of diagnostic information from various diagnostic tools (i.e. KPCA, sensor check module) to precisely diagnose the root cause of fault.
- Develop systematic methodology to build BN (i.e. causality network, conditional probability) utilizing process data.

The innovation behind this paper is how to combine the knowledge of individual methods in a hybrid framework. The main purpose is to develop a systematic hybrid tool for industrial fault detection, identification and diagnosis. The combination of some single methods has been less focused in the recent literature and is the novelty of this research.

1.3. Thesis structure

The rest of this thesis is organized as follows: the second chapter will briefly describe fault detection and diagnosis methods and will highlight the most relevant sections related to the main objective of this thesis. In the third chapter, combination of KPCA and causality analysis was implemented to detect industrial faults and qualitatively diagnose the root cause. In the fourth chapter, a hybrid method combining KPCA and Bayesian network was implemented for fault detection and diagnosis, also some implementation issues of Bayesian network which received less research were addressed in this chapter. Finally, in chapter five research findings were summarized and some future research directions were discussed.

Chapter 2

Literature review

2.1. Background

Today's plants in chemical and petrochemical industries are becoming larger, more complex, and operate with a large number of variables under closed-loop control. As industrial systems enlarge, the total amount of energy and material being handled increases. Corollaries of this trend imply that each hour of down-time is more expensive, and that the source of malfunction or fault is more difficult to locate. Fault is defined as "an unpermitted deviation of at least one characteristic property of a variable from an acceptable behavior" according to Isermann [8]. Faults in a system may lead to degraded performance, malfunctions, or failures. The consequences of a failure are usually more serious, such as partial or complete system breakdown [9]. Therefore, early and correct fault detection and diagnosis is imperative both from the viewpoint of plant safety as well as reduced manufacturing cost. By process monitoring it is possible to reduce occurrence of sudden, disruptive, or dangerous outages, equipment damage, and personal accident, and to produce higher quality products [3].

2.2. Fault detection and diagnosing the root cause of the fault

Fault is malfunction of a system component and includes instrument malfunction (sensor or actuator) and abnormality due to variation in process internal variables. Instrument malfunction cannot be propagated through the process while variation in process internal states will be propagated through system and will affect the other states. The observable effect of a fault is symptom. Although the existence of noise is normal to a certain extent in a process, it always affects the symptoms and makes the task of process monitoring hard. The four procedures associated with process monitoring are: fault detection, fault identification, fault diagnosis and process recovery. Fault detection is determining whether a fault has occurred. Fault identification is identifying the observation variables most relevant to occurrence of the fault. Fault diagnosis is determining where fault occurred, in other words, determining the cause of the observed out-of-control status [3].

Methods of FDD methods can be broadly classified into two major categories: model based methods, and process history based methods. Model based methods are divided to qualitative and quantitative sections [1, 4, 10]. Here we briefly explain these methods (Fig. 2.1).

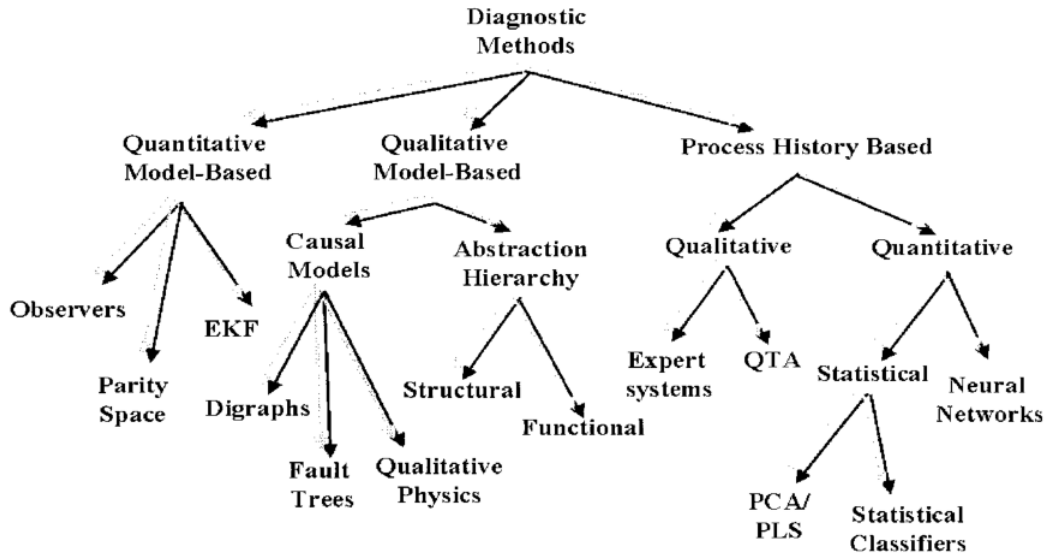


Figure 2.1. Fault diagnosis method (Venkatasubramanian, Rengaswamy et al. 2003)

2.2.1. Model- based fault detection and diagnosis

Model-based fault detection schemes are based essentially on analytical redundancy [11]. Sensor outputs are not independent from each other nor from the inputs to the system and given sufficiently accurate knowledge about a model representing the relationship between different variables in a process, the difference between the model outputs and the measurements are used to detect discrepancies. Clearly, model-based methods require an accurate analytical model of the system [10]. In general, a model based FDD system consists of two modules: residual generator and residual evaluator (Fig. 2.2). Residual generator compares the measurements of the system with the process model outputs and reports these differences as residuals. The residual evaluator receives the residuals and makes decision about faulty or normal state of the process [12]. Many model-based methods involve linearizing the model (if it is non-linear) about an operating condition in a narrow range and putting it into state space form (continuous or discrete), then calculating a residual vector from the measurements. The size of the residual can be compared to

a threshold to determine if a fault has occurred. Other properties of the residual vector are then evaluated to determine the type and magnitude. This can be accomplished by either designing the residual generation such that each element of the residual vector corresponds only to one particular fault, or by comparing the direction of the residual vector to the direction expected for each fault [13].

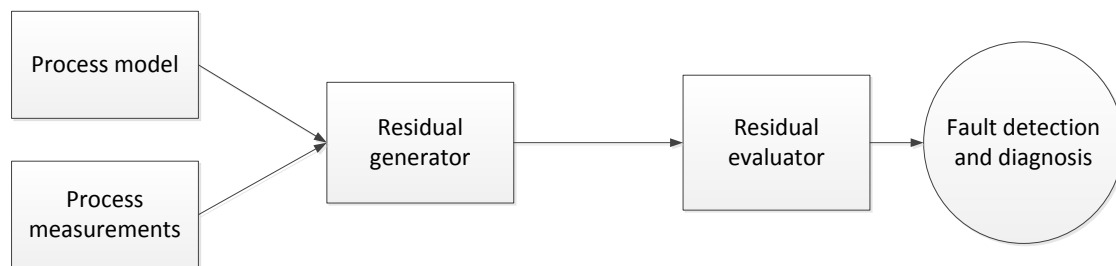


Figure 2.2. Model based fault detection strategy [13]

In 1976, Willsky wrote the first major survey paper on model based FDD [14], especially on linear time invariant systems. This is followed by Isermann where he reviewed FDD design based on modeling and estimation method [13]. In 1988, the main properties of model based FDD was explained by Gertler where he presented the robustness and sensitivity considerations [15]. Frank developed an algorithm based on Artificial Intelligence-based FDD [16]. The offline and online algorithms in FDD was presented in a survey paper by Basseville [17].

Model based methods can be divided into qualitative model based methods and quantitative model based methods. In quantitative models the relationships between the inputs and outputs are expressed by mathematical functions [10]. They compare the outputs of the real system with the expected value to detect and diagnose the faults. In quantitative model-based methods, the purpose is to detect a fault in the processes, actuator and sensors by comparing the difference between model and the process measurements that is called residual [8]. The main challenge in this method

is how to express the process in a model that accurately and comprehensively show the dependency between different parameters. In addition, chemical engineering processes are often nonlinear, which makes the design of fault diagnosis procedures more difficult. Furthermore, due to the on-line requirements of the system, the implementation of the model-based fault diagnosis system strongly depends on the power of the computer system used. Thus, the rapid development of computer technology and control theory is a reason why the model-based fault diagnosis technique is becoming more accepted as a powerful tool to solve fault diagnosis problems in technical processes [20]. In qualitative models these relations are expressed by qualitative terms that are expressed either as qualitative casual models or as abstraction hierarchies for each unit in a process. In other words, it is in fact a knowledge base method that uses a set of if-then-else and inference engine to reach a conclusion [10] (more explanation is in section 2.2.3). Important reviews in the field of model-based methods include those by Chow and Willsky [21], Isermann [13], Basseville [17], Gertler and Singer [22], Frank [10], Isermann [11], Frank et al. [16], Isermann [8], Venkatasubramanian [10, 23].

2.2.2. Process history-based FDD

Process history based methods are based on a large amount of historical process data and use a priori knowledge to extract features. Process data collected from the normal and abnormal operating conditions are used to develop measures for detecting and diagnosing faults. Since these methods are data-driven, the effectiveness of these methods is highly dependent on the quality and the quantity of the process data. Although modern control system allow acquiring huge amount of process data, only a small portion is usable as it is often not certain these data are not corrupted and no unknown fault are occurring [4].

According to the extraction process, the methods are divided into quantitative and qualitative methods. Methods that extract qualitative information include expert systems and qualitative trend analysis (QTA). Quantitative methods include neural networks and statistically derived models. Statistical models include those based on principal component analysis (PCA)/partial least squares (PLS) [23].

Both types of the model-based and history-based approaches have their advantages and deficiencies. According to the comprehensive review of Venkatasubramanian and Iserman model-based FD can handle unexpected faults if complete knowledge of all inputs and outputs of the system including their dynamic relationships is available; however, in model-based FD such modeling information is not always available, and the modeling itself is not always accurate due to system complexities and nonlinearity. In contrast, data-driven FFD is easier to implement and thus widely selected for applications due to the lower requirement of a priori knowledge, while its performance yield to degradation by sensor failures and the limited coverage in the measurement space of the fault classifiers [4, 8].

In this thesis KPCA, which is nonlinear form of PCA, was used for detection of abnormality in a process. PCA is a multivariate analysis technique that extracts a new set of variables by projecting the original variables onto principal component space [24]. The extracted variables, called PCs, are linear combinations of the original variables in which the coefficients of the linear combination can be obtained from the eigenvectors of the covariance (or correlation) matrix of the original data. Geometrically, PCA rotates the axes of the original coordinate system to a new set of axes along the direction of maximum variability of the original data [25]. PCs are uncorrelated with each other, and the first few PCs can usually account for most of the information of the original data.

Determination of the appropriate number of PCs can be subjective. Several techniques exist for determination of the value of the reduction order like the percent variance test, the scree test, parallel analysis and the PRESS statistic [11, 26]. This method suffers from nonlinearity in the system data.

In process monitoring with PCA models, it is assumed that a monitored process behaves linearly; however, when a process is nonlinear, a linear PCA model might not perform properly. Much research in this area has been performed to find a nonlinear version of PCA. Principal Curves [27], Kernel PCA [28], Mixture of Probabilistic PCA [29], Input Training Neural Networks [30] and Gaussian Process Latent Variable Model [31] are some of the suggested methods for implementing nonlinear PCA. Some of these methods which has been used in process monitoring is kernel principal component analysis (KPCA) which maps measurements via a mapping function from their original input space to a higher dimensional feature space where PCA is performed. The mapping function should be selected carefully, because its type determines the accuracy of the linearization [32].

An important property of the feature space is that the dot product of two vectors Φ_i and Φ_j can be calculated as a function of the corresponding vectors x_i and x_j , this is,

$$\Phi_i^T \Phi_j = k(x_i, x_j) \quad (2.1)$$

The function $k(\cdot, \cdot)$ is called the kernel function, and there exist several types of these functions. Some popular kernel functions are polynomial functions; radial basis, or Gaussian, functions; and sigmoidal functions [28, 32]. More explanation on calculation detail on this section is provided in Appendix.

To illustrate how a nonlinear mapping to an expanded dimensional space can change a nonlinear distribution to a linear distribution, the following illustrative example is given: suppose we have a nonlinear process with two variables, x_1 and x_2 , and there are two data sets; one set has normal measurements and the other one faulty measurements. Fig. 2.3 shows the plots of these data sets; the normal measurements are marked with blue asterisks and the faulty ones with green dots. In this case it is impossible to apply linear PCA to separate the normal data from the faulty one. However, as shown in Fig. 2.3, if we add a third dimension to the plot, calculated as $x_1^2 + x_2^2$, it is really easy to separate the normal and faulty measurements with linear PCA. Therefore, even though the original data is nonlinear in a bi-dimensional space, its mapping to a tridimensional space is linear. Principal Curves [27], Mixture of Probabilistic PCA [29], Input Training Neural Networks [30] and Gaussian Process Latent Variable Model [31] are some of the other suggested methods for implementing nonlinear PCA. Some of these methods such as Kernel PCA (KPCA) and Principal Curves have been used for process monitoring [24, 33].

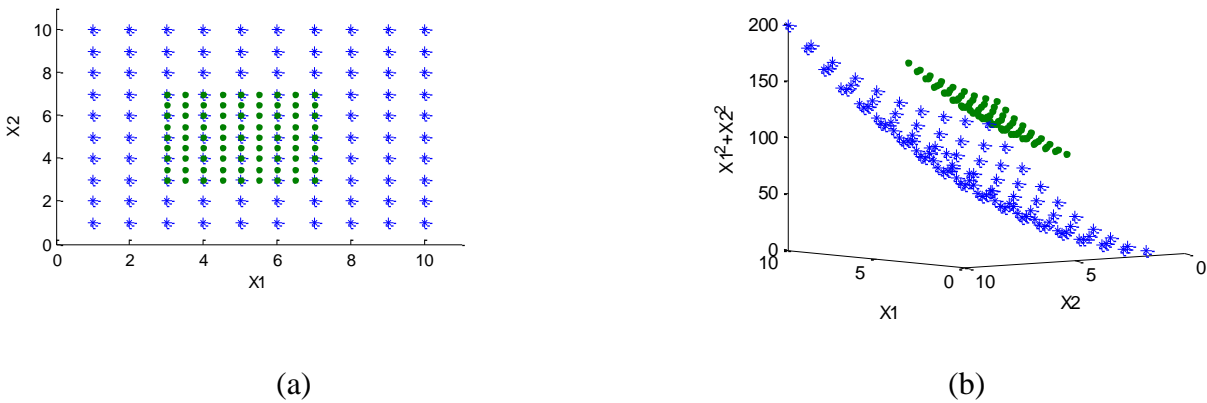


Figure 2.3. Normal and faulty data (a) nonlinear (b) linear (after applying kernel)

Although PCA and its derivatives are powerful tools among data-driven methods, they work appropriately in detection phase and isolate the variables that have high contribution in occurrence

of fault [4, 34]. The highly contributed variables based on contribution plots are those variables in the process that has high amount of variation due to occurrence of fault; however, the highest contributed variable in contribution plots is not always the true root cause of the fault which makes the task of fault diagnosis difficult. In diagnostic methods, there should be enough evidence on considering a suspected variable as the root cause of a fault. However, in PCA there is not enough evidence to diagnose the highly contributed variable as the true root cause of a fault. For example sensor fault diagnosis problem using PCA is studied by Dunia[35]. They have proved that the method of PCA filtering satisfies detection but since it does not satisfy the identifiability condition, they used an optimization approach to reconstruct the faulty data. In this method, the notion of Sensor Validity Index (SVI) is introduced. SVI is a number between zero and one. When a given sensor is healthy SVI is close to one and vice versa. So the faulty sensor is diagnosed; however, the problem still exist and this method cannot always find the faulty sensor. The reason is that some sensors are much more sensitive than others in a sensor array and therefore have more influenced to this kind of filtering. So this method needs to be combined with another technique which can conduct the diagnosis phase[36].

2.2.3. Knowledge base methods in FDD

2.2.3.1. Fault tree analysis

A fault tree analysis or FTA converts the physical system into a structured logic diagram in which the event symbols and logic symbols are used. FTA includes the following four steps: system definition, fault-tree construction, qualitative evaluation, quantitative evaluation [37]. Hessian et al. used a FTA to diagnose faults for an existing control-room HVAC system. This logic-based methodology was incorporated into the operating system design to improve system reliability [38].

2.2.3.2. Signed digraphs

A signed digraph or SDG uses graphical models to capture the root cause. A SDG is usually built by nodes and directed arcs, in which the nodes indicate state variables, failure origins and alarm conditions, and directed arcs show the relationship between these nodes. Shiozaki and Miyasaka developed a HVAC fault diagnosis tool using SDG. A real-time fault diagnosis system could be created using this tool [39]. Maurya et al. presented SDG methods which were used for safety analysis and fault diagnosis in chemical process systems [40].

2.2.3.3. The possible cause and effect graph

The possible cause-effect graph (PCEG) model consists of a representation of knowledge about a process and an inference strategy. The PCEG model is designed to take advantage of a large number of families of concepts. The model assumes that each family of concepts describes a partition of the plant time set and that one concept in each family represents the normal state of the process. [41].

As mentioned earlier, any diagnosis model captures certain features of diagnosis reasoning better than other diagnosis models. Some of the reasons which indicate that PCEG may be the appropriate model to use rather than another models include the need to include general partition, a potential which exists for varying set of measurements, first principle knowledge which exists about the process, existence of coupling or recycling, possibility of explanation of all scenarios, complexity of a system.

2.2.3.4. Bayesian network

Bayesian network can effectively characterize the complex causal relationships among variables of a system with stochastic uncertainty [42]. It visually represents a probabilistic relationship

among some variables that are related to each other by arcs [43]. The problems that have been solved with a BN include diagnosis, automated vision, sensor fusion, manufacturing control, transportation, ecosystem, environmental management and forecasting [44-47]. Suitability for small and incomplete data, ability to combine different kind of knowledge and sources, and network learning capability are among the advantage of using a BN [47]. A BN has both qualitative and quantitative parts [48]. The qualitative part is a directed acyclic graph consisting of hidden (happenings) and observed nodes (measurements) with statistical dependencies represented by the arcs connecting the various nodes [9, 49]. The nodes with arcs directed into them are termed as child nodes, whereas the nodes from which the arcs depart are parent nodes. The quantitative part is a Conditional Probability Table represents quantitatively the cause and effect among variables. The nodes without any parents are called root nodes. BN is in fact a couple (P, G) where:

P is a directed acyclic graph in which the nodes are random variables and some edges that represents conditional independent variables.

G is a set of conditional probability distributions for each node (or each variable) either may be a table, for discrete random variables, or distribution, for continuous random variables, although in practice only discrete and Gaussian random variables can be treated due to mathematical complexity of the other type of continuous distributions [9, 50]. Such a network is called Conditional Gaussian Network. In order to facilitate the computation in a Conditional Gaussian Network a discrete variable is not allowed to have a Gaussian variable as its parents [51-53].

The issue of distinguishing between sensor and process fault has recently been the matter of debate. Krishnamoorthy et al. used Bayesian network to determine if the abnormal behavior is due to

malfunction in the sensor or due to a process fault. They used the same network to both verifying the values of sensors and decision making [54]. Mehranbod et al. proposed a BN-based method for both single and multiple sensor fault detection and identification. They showed their method is capable of detection and identification of instrumental fault (bias, noise and drift) in both cases [55]. Dey et al. addressed the variation in tool wear, workpiece hardness and stock size in production machining environment and developed a methodology for diagnosing the root cause of process variation that are often confounded in process monitoring [56]. Yu et al. developed a modified Bayesian network-based two stage fault diagnosing methodology. They incorporated the result of Independent Component Analysis (ICA) and a Bayesian network for this aim [36]. More interesting was the work done by Yu et al. in which they used a dynamic Bayesian Network for all detection, identification and diagnosis phase. Abnormality likelihood index was introduced for detection of abnormal events. Bayesian contribution index was used for determination of contribution of each variable in abnormal event. The updating of network has lead to determination of fault propagation pathway in this work [57].

The network in a Bayesian network represents a causal relationship between different variables (nodes). Most research worked with Bayesian network for fault diagnosis construct the network based on process knowledge [36, 57]. However, one cannot be confident about constructed network based on knowledge of the process. More reliable network is the one that is constructed in corporation of both process knowledge and process data. Among the techniques that can be used for determining causality using process data are Granger causality and transfer entropy that will be explained more in the next chapters.

Despite the abundance of research in the diagnosing a fault via BN, it is still unclear how to train the network and calculate conditional probabilities. Also, there is still ambiguity whether one

should use normal or faulty data for network training [36, 57]. Except faults, raw data of a process contain all noise and normal process variations which are considered as normal states of the process. So the methodology which is trained with raw data will be sensitive even to normal variation of the process. There is less focus on whether we should use the raw data directly or we need some preprocessing on data before using them for training purpose. Also loop handling is a concern in applying Bayesian network for industrial process fault diagnosis. Since BN is an acyclic network, the updating of the network is not possible when it contains a cycle. However, in industrial processes there are many cycles such as close loop control system or reflux flow. This limits the application of BN in such a case.

2.3. Combined framework of fault detection and diagnosis

Currently there is no method that has all features of fault detection and diagnosis in a process. Each method has its own advantages and drawbacks [4]. Also some techniques perform appropriately in detection while others perform well in diagnosis phase [5, 6, 34]. To have a more complete technique by which both detection and diagnosis phase can be done, researchers have proposed hybrid framework in which a collection of methods are employed to construct a more robust package for fault detection and diagnosis. This package brings the advantages of the single methods and overcomes some of the shortcomings of individual methods. This combination of different methods allows one to evaluate different kinds of knowledge in one single framework for better decision making [7].

A hybrid approach for fault detection in nonlinear systems was proposed by Alessandri [58]. They used some estimators, which provides estimation of parameters which describe instrumental faults, for fault detection and isolation. The estimators were designed using an optimal estimation

function which are approximated feedforward neural networks and the problem is reduced to find the optimal neural weights. The learning process of the neural filters is split into two phases: an off-line initialization phase using any possible "a priori" knowledge on the statistics of the random variables affecting the system states, and an on-line training phase for on-line optimization of neural weights. The approach proposed by Alessandri is only a fault detection and isolation method, leaving fault identification problem unsolved. A hybrid robust fault detection and isolation in a nonlinear dynamic systems was proposed by Xiaodong et al [59]. They utilized some adaptive estimators for this purpose. The fault detection and approximation estimator (FDAE) has been used to detect the fault, and the remaining estimators which are fault isolation estimators (FIEs) were used for isolation of faults. In other words, under normal operating conditions (without faults) FDAE is monitoring the system to distinguish whether the system is working under normal or faulty state. Once a fault is detected, the bank of FIEs is activated for isolation purpose. The nominal mathematical model of the system is explicitly used for designing both FDAE and FIEs. Recently, Talebi et al. proposed a hybrid intelligent fault detection and isolation methodology using a neural network- based observer. The advantage of their method is that it does not rely of the availability of full state measurements [60]. In order to make fault effect clearer and recognizable, Ren et al. proposed a combined method of wavelet transform and neural network. They used multi-scale wavelet transform to prolong the effect of fault in residuals before feeding them to neural network [61]. Mylaraswamy provided a brief comparison of the various diagnostic methods to highlight the inadequacy of individual methods and motivate the need for collective problem solving [6]. Mallick et al. proposed a hybrid method of PCA and Bayesian network to this purpose. They used PCA in diagnosis phase and probabilistic Bayesian network in diagnosis phase [34]. This framework for collective problem solving has been the focus of some researchers.

Chen et al. proposed a wavelet-sigmoid basis neural network for dynamic diagnosis of failure in hydrocracking process [5]. However there is still more need to research in this area especially since it is somehow unclear how to use the outcome of first section as an input to the other section. In other words it is worthwhile to know how to combine the knowledge of individual methods in a hybrid framework.

As mentioned earlier, currently there is no single diagnostic method or technique which is superior to all other techniques. Each method manages to capture or model some subset of the features of the diagnostic reasoning and thus may be more suitable than other techniques for a particular class of problems [5]. In such a case hybrid frameworks consisting of a collection of methods performing cooperative problem solving is proposed as an alternative to individual methods. Such a hybrid framework will be an effective way of utilizing all available information and overcoming limitations of individual methods [4, 6, 7]. This combination of different methods allows one to evaluate different kinds of knowledge in one single framework for better decision making. This is the novelty and the main contribution of this thesis which will focus on how to use information of some diagnostic methods in other diagnostic methods. However, based on the reviews literature, there are some gaps in diagnostic task. Some of these gaps are related to the network constructed for failure diagnosis which have been explained in section 2.2.3.4. Another problem is how to distinguish sensor failure from the failures which is related to process internal states. All these concern will be addressed in this thesis.

Chapter 3

Combination of KPCA and causality analysis for root cause diagnosis of industrial process fault

Abstract: Kernel principal component analysis (KPCA) based monitoring has good fault detection capability for nonlinear process data, however it can only isolate variables that have contribution in occurrence of fault and thus not precise in diagnosing. Since there is a cause and effect relationship between different variables in a process, accordingly a network based causality analysis method was developed for different fault scenarios to show causal relationship between different variables and to see the causal effect between the most contributing variables in occurrence of fault. It was shown that KPCA in combination with causality analysis is a powerful tool for diagnosing the root cause of a fault in the process. In this paper the proposed methodology was applied to Fluid Catalytic Cracking unit and Tennessee Eastman process to diagnose root cause for different faulty scenarios.

Keywords: kernel principal component analysis (KPCA), causality analysis, transfer entropy, fluid catalytic cracking.

3.1. Introduction

Rapid development in industry have contributed to more complex systems that are prone to risk of failure, which are inevitable in any kind of industrial systems [23, 62]. In applications where the presence of faults may lead to premature failure, increased operating costs, or other undesirable consequences, fault detection and diagnostics (FDD) tools are often implemented [4]. The objectives of these tools are earlier detection of problems and expedited corrective action that minimize the fault's impact on the system [3]. For the purpose of FDD, no single method has all the desirable features and each of them deals with some limitations [4]. In such a case, hybrid frameworks consisting of a collection of methods performing cooperative problem solving is proposed as an alternative to individual methods. Such hybrid framework is an effective way of utilizing all available information and overcoming limitations of individual methods. This combination of different methods allows one to evaluate different kinds of knowledge in one single framework for better decision making [7].

The work of Venkatasubramanian and Rich is among the earliest research in hybrid framework. In order to achieve an efficient diagnostic tool without scarifying the flexibility and reliability, they integrated the process knowledge with rule-based approach in an object-oriented two-tier methodology in which the process specific knowledge is in top-tier and the process rule-based knowledge is in bottom-tier. The proposed diagnostic tool was able to identify the potential suspects [63]. The analytical methods in model-based fault detection and diagnosis are based on residual generation using parameter estimation; however, the robustness of the model-based methods is often under question since obtaining an accurate model for process, especially for chemical processes, is problematic. To address this problem, Frank proposed the use of analytical methods and integrated them with knowledge-based methods. They concluded knowledge-based

methods (expert systems) complement the analytical methods of fault diagnosis [16]. An integration of neural network and expert system for fault diagnosis was done by Becraft et al. Once the process fault was diagnosed by neural network, the results was analyzed by a deep knowledge expert system to recover the process [64]. The use of hybrid methods became common and in 1997 Mylaraswamy provided a brief comparison of the various diagnostic methods to highlight the inadequacy of individual methods and underscore the need for collective problem solving. They proposed a Dkit based hybrid method of neural network for detection of a fault and a SDG for diagnostic action [6]. Zhao et al proposed a wavelet-sigmoid basis neural network for dynamic diagnosis of failure in hydrocracking process [5]. A hybrid methodology consisting of PCA and a Bayesian network was done in which PCA was conducted for earlier fault detection and Bayesian network was implemented for the isolation of the fault [34]. However there is still more need for research in this area especially since it is somewhat unclear how to use the outcome of some diagnostic tools as an input to the other tools. The innovation behind this paper is how to combine the knowledge of individual methods in a hybrid framework. The main purpose is to develop a systematic hybrid tool for industrial fault detection, identification and diagnosis. In the proposed methodology we combine kernel principal component analysis (KPCA) and PCA with two different causality analysis techniques namely, transfer entropy and Granger causality respectively. We also address how to use these causality analysis tools as qualitative techniques for root cause diagnosis of a fault in real practical processes which have not been focused in literature. In the next section we describe the methodology with instruction for coupling these techniques. The rest of this paper is organized as follows: the second part will briefly explain KPCA, transfer entropy and Granger causality and will provide a mathematical example to compare the results of transfer entropy and Granger causality. In the next section the application

of proposed method on FCC and Tennessee Eastman Chemical process is described. Finally, we conclude the paper with some concluding remarks and directions for future research.

3.2. Methods and techniques

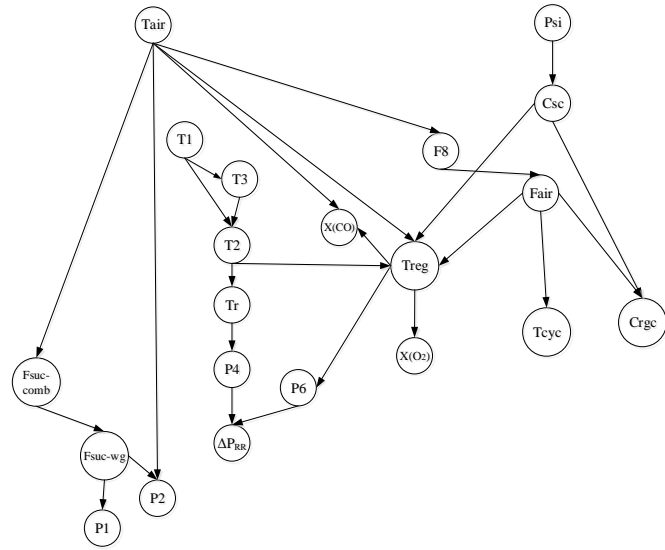
As one of the most popular statistical methods, PCA extracts usable information from raw data [3]. Though originally developed to reduce the dimensionality of data, PCA is appropriate for fault detection. For diagnosing the main root cause, PCA is not an accurate tool but still the contribution plots based on PCA are worthwhile for identification of some of the variables that has the most effect on the occurrence of the fault [65]. However, PCA is not optimal when the data of a process does not follow a linear trend. KPCA is better suited to deal with process nonlinearity. On the other hand, causality analysis techniques between process variables have been the interest of research [66]. Among these techniques Granger causality and transfer entropy are prevalent methods to ascertain the causal relationship between process variables [67, 68]. The idea of causality analysis was first introduced by Granger in 1969. According to Granger, a variable 'X' Granger causes the other variable 'Y', if incorporating the past values of 'X' and 'Y' helps to better predict the future of 'Y' than incorporating the past values of 'Y' alone [69]. The notion of Granger causality has been applied in the study of numerous economic relationships including that between money and prices, wages and prices, exchange rates and money supply, and money and income [70]. The transfer entropy provides a wide variety of approaches for measuring causal influence among multivariate time series [71]. Based on transition probabilities containing all information on causality between two variables, the transfer entropy approach was proposed to distinguish between driving and responding elements [72], and is suitable for both linear and nonlinear relationships; it has been successfully used in chemical processes [73] and neurosciences [74].

Although PCA and KPCA are powerful tools for detection of a fault in a system, it cannot precisely identify the root cause. On the other hand transfer entropy or Granger causality can determine the cause and effect relationship between variables in a process; however, they suffer from the complexity of calculation when too many variables are involved in the calculations [71]. Also when there are too many variables, the constructed network based on causality analysis will be complex and busy and it does not give enough evidence to qualitatively identify the root cause of a fault (Fig. 3.1- a and b). The general considerations in application of PCA, KPCA, Granger causality and transfer entropy and their drawbacks are given in Table 3.1. Taking the considerations of each of these individual methods into account, this paper proposes a hybrid method of fault detection and diagnosis in industrial processes. Based on this table, a good combination between these methods will be done by combining PCA with Granger causality for detection and diagnosis of a fault in a linear system and also by combining KPCA with transfer entropy for detection and diagnosis of a fault in a nonlinear system. Since most of practical process data is nonlinear, it is better to combine KPCA for detection of a fault with transfer entropy as a causality tool for diagnosis. In this paper, additionally, even for nonlinear data we use Granger causality as one of the other tools for causality analysis for two reasons. First, based on some literature it has been theoretically proved that when data has normal distribution, Granger causality and transfer entropy has the same results [75, 76]; however, there is no practical case study to show this in a real system. Besides the main objective of this paper which is root cause diagnosis of process faults, one of the other interesting objectives is to show equivalency of Granger causality and transfer entropy in some real case studies. Secondly, the original Granger causality method which is proposed by Granger is linear. Linear Granger causality has low power to show the causal effect between variables in a nonlinear system. A nonlinear Granger causality developed by

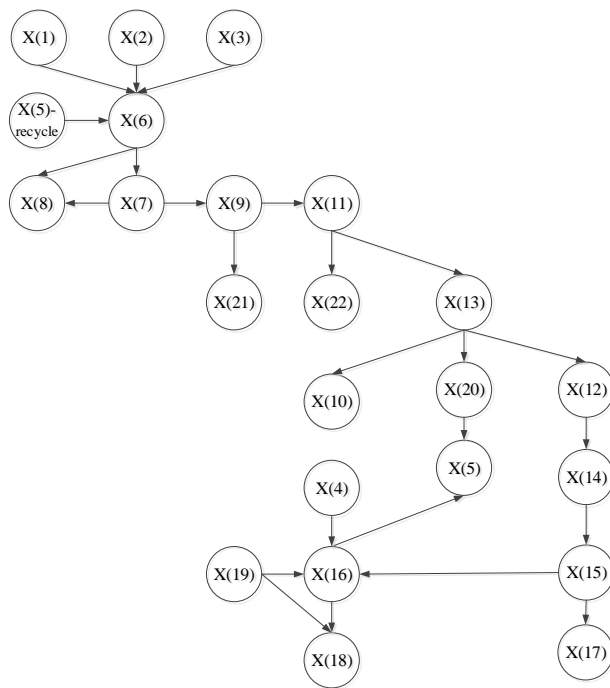
Hiemstra and Jones [77] to examine the dynamic relation between variables of stock markets but their test was questioned by Diks and Panchenko [78]. As a result, the nonlinear application of Granger causality is still under question. So in this paper, we use both transfer entropy and Granger causality as two tools of causality analysis and will compare their performance on two case studies. Fig. 3.2 illustrates the procedure in which first KPCA was applied on the data gathered from the process. The KPCA detects the fault and identifies the variables which have the most contribution. In the diagnoses phase, causality analysis was performed among those most likely variables contributing toward the fault, and a simple network was constructed which provides a straightforward estimation of the root cause of the failure. Causality analysis can be done either by Grange causality and transfer entropy method. By combining KPCA and causality analysis the combined framework is a more complete package for FDD in comparison to each individual method.

Table 3.1. General consideration of process monitoring tools

	Linear/ nonlinear	Calculation	Detection/diagnosis
PCA	Linear	Simple	Detection
KPCA	Nonlinear	Complex	Detection
Granger causality	Linear	Simple	Diagnosis
Transfer entropy	Linear/nonlinear	Complex	Diagnosis



(a)



(b)

Figure 3.1. Causality network of (a) Fluid Catalytic Cracking process (b) Tennessee Eastman Chemical Process

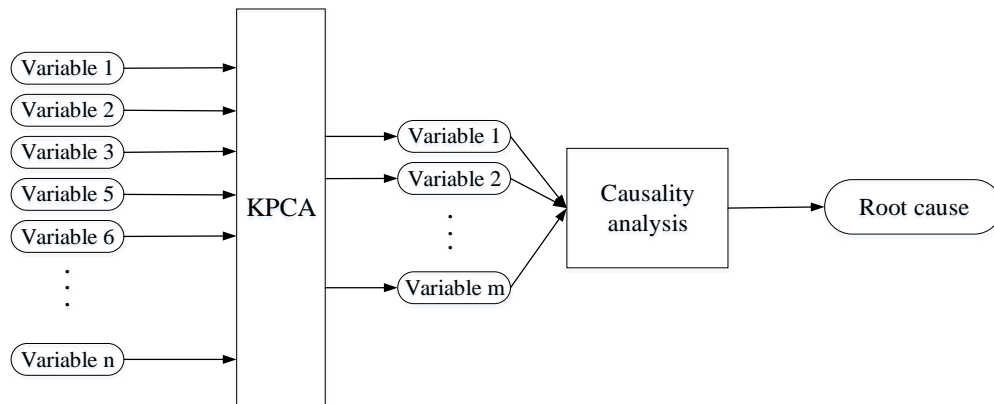


Figure 3.2. Schematic illustration of the proposed FDD method

3.2.1. Kernel Principal Component analysis (KPCA)

PCA is a multivariate analysis technique that extracts a new set of variables by projecting the original variables into principal component space. The extracted variables, called PCs, are linear combinations of the original variables in which the coefficients of the linear combination can be obtained from the eigenvectors of the covariance (or correlation) matrix of the original data [79]. Geometrically, PCA rotates the axes of the original coordinate system to a new set of axes along the direction of maximum variability of the original data [25]. PCs are uncorrelated with each other, and the first few PCs can usually account for most of the information of the original data [3].

In process monitoring with PCA models, it is assumed that a monitored process behaves linearly. However, in most practical scenarios chemical processes are nonlinear, as such a linear PCA model is not optimal for fault detection. According to Cover's theorem, the nonlinear data structure in the input space is more likely to be linear after high-dimensional nonlinear mapping (Fig. 3.3) [79]. KPCA exploits this property and projects data in higher dimensional space, subsequently PCA is

applied on the correlation matrix of the transformed variables. For example, a data set x is transformed into the feature space through mapping function Φ . The covariance of the mapped data is $\Phi(x) \cdot \Phi(x)$.

Φ is the mapping function which is usually not easy to determine [80]. Since only the dot product is required in the transformed space, an alternative is to use a kernel function $k(\cdot, \cdot)$ which can provide the dot product without the explicit mapping function as in Equation 3.1.

$$k(x, x) = \Phi(x) \cdot \Phi(x) \quad (3.1)$$

There exists several types of these functions. Some popular kernel functions are polynomial functions; radial basis, or Gaussian functions; and sigmoidal functions [28, 32].

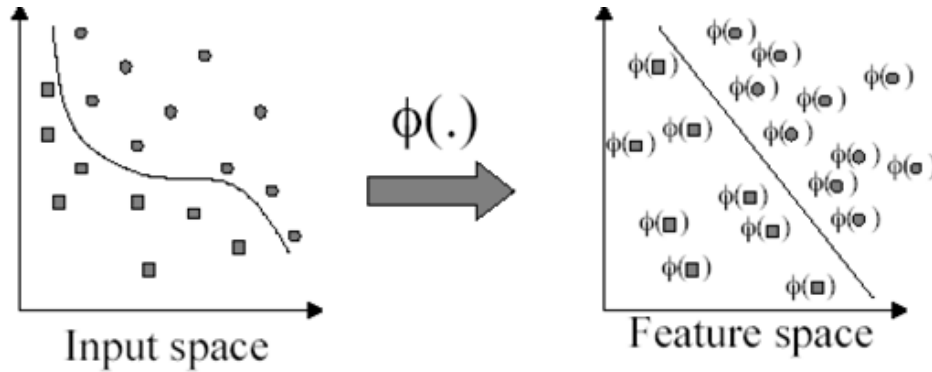


Figure 3.3. Linearization with mapping function in KPCA

3.2.2. Causality analysis based on Granger Causality

Granger causality uses parameters from an (Auto Regressive) AR model fit to the system in question. A general form of the AR model which is used in system model prediction is shown in the following equation:

$$x_t = \sum_{i=1}^r \alpha_i x_{t-i} + e_t \quad (3.2)$$

Where x is a vector consisting r time series data points; α is a $r \times r$ coefficient matrix and e is the uncorrelated noise vector. The concept of the history-based causality introduced by Wiener and formulated by Granger has played a significant role in investigating the relations among the stationary time series [69, 81]. The original definition by Granger, which is called Granger Causality, refers to the improvement in predictability of a time series x that derives from the incorporation of the past of x itself and another series y , above the predictability based solely on the past of the x series [69]. Considering two time series x and y , there are two different linear regression model. One is a restricted model in which the prediction of x at time k is possible using the information of the past of x :

$$x_k = \sum_{i=1}^p \mu_i x_{k-i} + \varepsilon_{xk} \quad (3.3)$$

where x_k is the x time series at time k ; x_{k-i} is the i -lagged x time series; μ is the regressive coefficients; p is the amount of lag considered; and ε denotes the residual series for constructing x_k .

The second model is unrestricted model in which the prediction of x at time k is done using the past information of both x and y as follows:

$$x_k = \sum_{i=1}^p \gamma_i x_{k-i} + \sum_{j=1}^q \beta_j y_{k-j} + \eta_{xk} \quad (3.4)$$

where x_k is the x time series at time k ; x_{k-i} and y_{k-j} are respectively the i -lagged x time series and j -lagged y time series; γ and β are the regressive coefficients; p and q are the amount of lag considered or model order; and η denotes the unrestricted model residual at time k . The μ , β , and γ parameters are calculated using least square method. In order to estimate the model, a small value of model order p results a poor estimation while a large value leads to problem of overfitting. Two

criteria are used to determine the model order namely, Akaike information criterion (*AIC*) [82] and Bayesian information criterion (*BIC*) [83]. For n variables, *AIC* and *BIC* are given as follows:

$$AIC(p) = \ln(|\Sigma|) + \frac{2pn^2}{T} \quad (3.5)$$

$$BIC(p) = \ln(|\Sigma|) + \frac{\ln(T)pn^2}{T} \quad (3.6)$$

where Σ represents the noise covariance matrix and T is the total number of observations. When the variability of the residual of the unrestricted model is significantly reduced with that of a restricted model, then there is an improvement in the prediction of x due to y . In other words y is said to Granger cause x . This improvement can be measured by the F statistic:

$$F = \frac{(RSS_r - RSS_{ur})/q}{RSS_{ur}/(T-p-q-1)} \sim F(p, T-p-q-1) \quad (3.7)$$

where RSS_r is the sum of the squares of the restricted model residual, RSS_{ur} is the sum of the squares of unrestricted model residual, and T is the total number of observations used to estimate the model. F statistics approximately follows F distribution with degrees of freedom p and $(T-p-q-1)$. If the F statistic from y to x is significant, then the unrestricted model yields a better explanation of x than does the restricted model, and y is said to Granger cause x [84].

3.2.3. Causality analysis based on Transfer entropy

For two process variables with sampling interval of τ , $x_i = [x_i, x_{i-\tau}, \dots; x_{i-(k-1)\tau}]$ and $y_i = [y_i, y_{i-\tau}, \dots, y_{i-(l-1)\tau}]$, transfer entropy from y to x is defined as follows [71]:

$$t(x|y) = \sum_{x_{i+h}, x_i, y_i} P(x_{i+h}, x_i, y_i) \cdot \log \frac{P(x_{i+h} | x_i, y_i)}{P(x_{i+h} | x_i)} \quad (3.8)$$

where P denotes the probability density function (PDF) and h is the prediction horizon.

Transfer entropy represents the measure of information transfer from y to x by measuring the reduction of uncertainty while assuming predictability [71]. It is defined as the difference between the information about a future observation of x obtained from the simultaneous observation of past values of both x and y , and the information about the future of x using only past values of x . The parameter values specially k , l , τ and h should be obtained based on several results and their comparison [68].

Using the above definitions, direction and amount of information transfer from x to y is as follows:

$$t(x \rightarrow y) = t(y|x) - t(x|y) \quad (3.9)$$

If $t(x \rightarrow y)$ is negative then information is transferred from y to x . Since at first there is no knowledge about which node is cause and which one is effect, choosing these nodes inversely will result in negative value.

The advantage of using transfer entropy is that it is a model free method and can be applied to non-linear data. It has already been proved to be very effective in capturing process topology and process connectivity. But it suffers from a large computational burden due to the calculation of the PDFs [71]. Non parametric methods, e.g. kernel method, can be used to estimate the PDF [85].

The Gaussian kernel function is used to estimate the PDF which is defined as follows [68]:

$$K(v) = \frac{1}{\sqrt{2\pi}} e^{-\frac{1}{2}v^2} \quad (3.10)$$

Therefore, a univariate PDF can be estimated by,

$$p(x) = \frac{1}{N.d} \sum_{i=1}^N K\left(\frac{x-x_i}{d}\right) \quad (3.11)$$

where N is the number of samples, d is the bandwidth chosen to minimize the error of estimated PDF. d is calculated by $d = c.\sigma.N^{0.2}$ where σ is variance and $c = (4/3)^{0.2} \approx 1.06$ according to the

“normal reference rule-of-thumb” approach. For a q -dimensional multivariate case the estimated PDF is given by [68]:

$$P(x_1, x_2, \dots, x_q) = \frac{1}{N \cdot d_1 \dots d_q} \sum_{i=1}^N K\left(\frac{x_1 - x_{i1}}{d_1}\right) \cdot K\left(\frac{x_q - x_{iq}}{d_q}\right) \quad (3.12)$$

where $d_s = c \cdot \sigma(x_{i,s})_{i=1}^N \cdot N^{-1/(4+q)}$ for $s = 1, \dots, q$.

3.2.4. Mathematical example on causality analysis

A simple mathematical model is used to investigate the applicability of mentioned causality analysis, i.e. Granger causality and transfer entropy. Assume four correlated continuous random variables x , y , z and w satisfying:

$$\begin{aligned} y_{k+1} &= 0.8 x_k + v_{1k} \\ z_{k+1} &= 0.6 y_k + v_{2k} \\ w_{k+1} &= 0.6 y_k + v_{3k} \end{aligned} \quad (3.13)$$

where $x \sim N(0,1)$; v_1 , v_2 and $v_3 \sim N(0,0.1)$; and $y(0)=2.8$. The simulation data set consists of 1000 samples. Based on the mathematical relation between variables the causal network is shown in Fig. 3.4 and this network will be validated by the above mentioned methods.

3.2.4.1. Validation by Granger causality

In order to test Granger causality between variables, the time series should be stationary, i.e. statistical properties such as mean, variance, and autocorrelation all are constant over time. *Eviews* was used to see the cause and effect relationship between x , y , z and w . *Eviews* is a statistical software used to analyze time-series oriented problems. The results are shown in Table 3.2. When $prob < 0.05$ the corresponding variable in that row has influence on the variable in the column. For

example $prob_{x \rightarrow y} = 0.0000$. It means that x has influence on y , consequently, there is an arc from x to y . Also $prob_{y \rightarrow z} = 0.0000$ and $prob_{y \rightarrow w} = 0.0000$ indicating arcs from y to z and y to w in the network.

3.2.4.2. Validation by transfer entropy

Transfer entropy was used to calculate mutual transfer entropy between all nodes. A Matlab code was developed for calculations. While calculating the $TE_{i \rightarrow j}$, multiple j -delays were given and the peak value of transfer entropy was considered over the delay (Table 3.3). The $TE_{x \rightarrow y} = 0.25$ indicating that x has influence on y . Also $TE_{y \rightarrow z} = 0.56$ and $TE_{y \rightarrow w} = 0.54$ indicating the arcs from y to z and y to w (Fig. 3.4). The calculation of probabilities in Equation 10 was done using histogram and it deals with some inaccuracy. Here a threshold of 0.1 was selected, thus the causal relationships between other variables were neglected and, consequently, the original network of the mathematical example will be verified in Fig. 3.4.

Thus it is obvious, when variables are following a normal distribution, the Granger causality and transfer entropy are showing the same causal relationship in network construction. This has been verified by other researchers as well [75, 76].

Table 3.2. Granger causality test results for mathematical model

	x	y	z	w	
x	-	59226.84	6.1749	1.6337	Chi-sq
	-	0.0000	0.0956	0.0741	Prob.
y	1.3044	-	479.75	439.20	Chi-sq
	0.5209	-	0.0000	0.0000	Prob.
z	1.4758	0.6921	-	0.0686	Chi-sq
	0.4761	0.7074	-	0.9663	Prob.
w	0.8374	1.0960	5.7775	-	Chi-sq
	0.6579	0.5761	0.0556	-	Prob.

Table 3.3. Mutual transfer entropy values for mathematical model

	x	y	z	w
x	-	0.25	<0.1	<0.1
y	-	-	0.56	0.54
z	-	-	-	<0.1

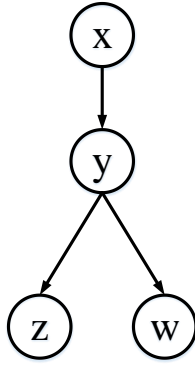


Figure 3. 4. The network of mathematical example

3.3. Industrial case studies

3.3.1. Fluid Catalytic Cracking Unit (FCC)

A FCC unit converts a number of heavy hydrocarbons with different molecular weights to lighter and more valuable hydrocarbons. The heavy hydrocarbons come from different parts of refinery and are diverse in chemical properties. FCC process was selected as one of the examples for this research. A schematic illustration of the FCC reactor/regenerator unit is shown in Fig. 3.5. There are three inputs to the system: fresh feed temperature, feed coke factor and ambient temperature. Also 20 variables are monitored during the process that all are shown in Table 3.4. Feed coke factor was considered to be 1.05 in all simulation studies. Therefore, two disturbances were introduced as faults to the system according to Table 3.5 [86].

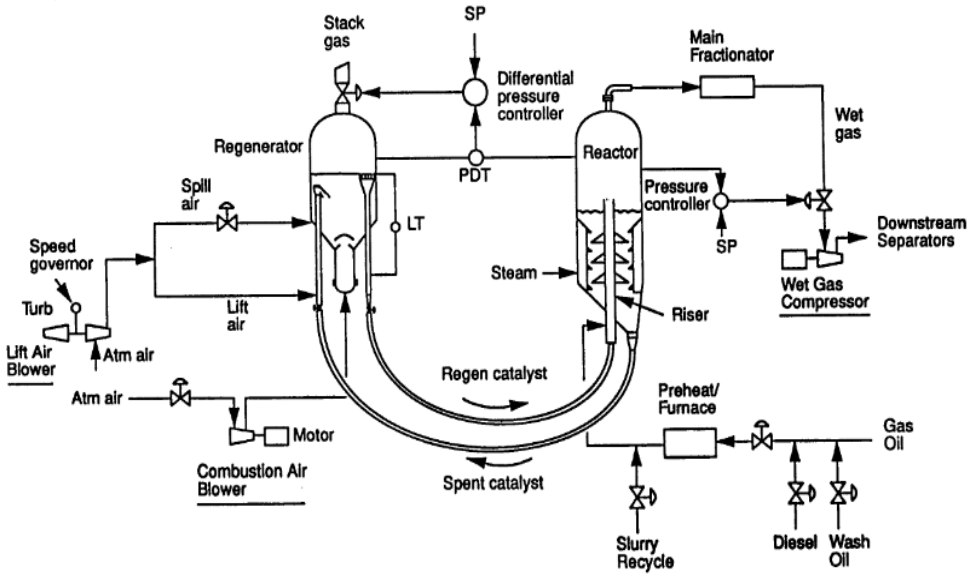


Figure 3.5. Schematic illustration of FCC process

Table 3.4. Measured variable of FCC process

No.	Variables	symbol
1	Ambient air temperature	T_{amb}
2	Fresh feed temperature	T_1
3	Effective coking factor	P_{si}
4	Reactor pressure	P_4
5	Differential pressure	ΔP_{RR}
6	Air flow rate into generator	F_{air}
7	Regenerator pressure	P_6

8	Furnace temperature	T_3
9	Preheated feed temperature	T_2
10	Riser temperature	T_r
11	Regenerator temperature	T_{reg}
12	Spent catalyst level	L_{sp}
13	Cyclone temperature	T_{cyc}
14	Differential cyclone temperature	DP
15	Stack gas CO concentration	X_{co}
16	Stack gas O ₂ concentration	X_{O_2}
17	Coke wt fraction in spent catalyst	C_{sp}
18	Coke wt fraction in regenerator	C_{rgc}
19	Air blower flow inlet-surge	F_8
20	Wet compressor inlet suction flow	$F_{sucn,wg}$
21	Combustion air suction flow	$F_{sucn,comb}$
22	Combustion air suction pressure	P_1
23	Combustion air discharge pressure	P_2

Table 3.5. Fault scenarios in FCC

Scenario No.	Fault description
1	5°C in atmosphere temperature
2	Gradual increase of 10°C in fresh feed temperature

In order to demonstrate the effectiveness of the proposed hybrid technique of KPCA and causality analysis, KPCA was used to detect the occurrence of fault. A training data set consisting of 1000 samples gathered under normal operating condition is used to develop KPCA model and estimate the Hotelling T^2 . In order to build the KPCA model, the values of the 23 variables in the FCC process were normalized around the Zero by standard deviation. The sampling time of the data is 1 second and a Gaussian kernel function was selected. Five principal components were selected that show 85% of the variations in the system. Only the eigenvectors and eigenvalues corresponding to selected PCs were considered. The threshold value based on normalized training data for Hotelling T^2 was calculated as 9.71 at 95% confidence level.

First abnormal event: The first faulty scenario begins with normal operation for 1000 seconds and then is followed by a 5°C increase in ambient air temperature for the remaining 4000 seconds.

The Hotelling T^2 and contribution plots of the KPCA analysis are shown in the Fig. 3.6. On Fig. 3.6a, the Hotelling T^2 shows the departure of variables from normal condition. This plot depicts a successful detection of this fault. As can be seen, there is a delay associated with the detection phase. It is because the magnitude of fault in ambient air temperature is not big enough to affect the process in a short time. Once these faults are detected, it is desired to isolate the occurred fault,

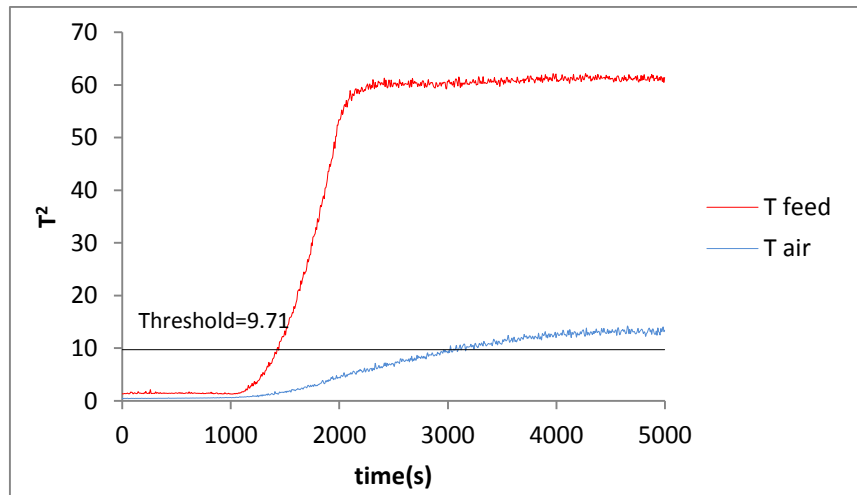
i.e. to identify those variables that are most correlated with occurred faults. Fig. 3.6b shows contributions of each variable in the fault occurrence. The calculation of contribution of each variables is calculated based on the method proposed by Alcalá and Qin [87, 88]. The contribution plots are based on average of contribution of all samples when the process is in abnormal state. It is obvious in this figure when there is a disturbance in ambient temperature, the other variables will be affected by this variation; however some variables will be affected more than others. It should be noted that the air enters to the regenerator through two air blower. One is a lift air blower that assists in catalyst circulation from the reactor to the regenerator. The other is a combustion air blower that provides the bulk of air required by the regenerator. So one expect that a variation in the ambient air temperature will mostly deviate the process in the regenerator side. This can be verified by the contribution plot since based on this plot, the following variables have significant contribution to the fault which all are in regenerator side:

- Ambient air temperature
- Regenerator pressure
- Combustion air suction flow
- Combustion air discharge pressure

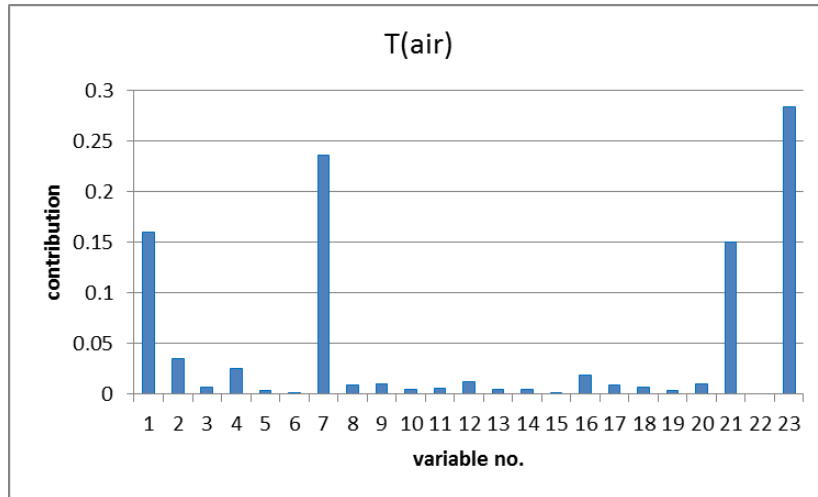
As the FCC process has 23 variables, it is difficult to decide about the root cause of a fault via the whole network containing all 23 nodes. The calculation of Granger causality and transfer entropy will be more complex when there are more variables. Even after doing such calculations, the constructed network was found too busy for visual illustration of the propagation path of the fault and diagnosing the root cause. The full network of FCC process is shown in Fig. 3.1a. It is obvious that the network is complicated and it is difficult to have an accurate estimation of the root cause

of the fault using this network. Hence, KPCA was used to narrow down the problem and to screen the most significant variables for further analysis. In fault diagnosis phase, the purpose is to investigate the cause and effect relationship between the variables selected by contribution plot. Table 3.6a shows the results of Granger causality test for this scenario for the selected variables via KPCA. Where the $prob < 0.05$, it rejects the null hypothesis and indicated that the variable in the row has influence on the variable in column. For example, based on the first column of Table 3.6a no variable has effect on ambient air temperature. In the second column, ambient air temperature has influence on regenerator pressure. Also in the third column of this table, ambient air temperature and combustion air suction flow have influence on combustion air discharge pressure and based on the fourth column ambient air temperature has influence on combustion air suction flow. These results are in accordance with the results of transfer entropy test. The mutual transfer entropy values were calculated among the most important variables as determined by KPCA contribution plots and the results are shown in Table 3.7a. In this table, when the value of transfer entropy is positive, the variable in row has influence on the variable in column and when the value of transfer entropy is negative, the variable in column has effect on the variable in the row. For example according to Table 3.7a ambient air temperature has effect on regenerator pressure ($TE_{T_{atm} \rightarrow P_6} = 0.13$). This is because variation in air temperature will affect the air density which is flowing to compressor and this compressor is adjusting the pressure inside the regenerator (P_6). On the other hand, combustion air suction flow has effect on combustion air discharge pressure ($TE_{F_{suctn,comb} \rightarrow P_2} = -0.25$) that is clearly interpretable based on process flow diagram. Among all 23 variables on FCC, the contribution plots of KPCA guide our focus more on the variables on a particular part of the process or among more important variables related to the fault, and causality analysis show the causal relationship between the variables in that particular part.

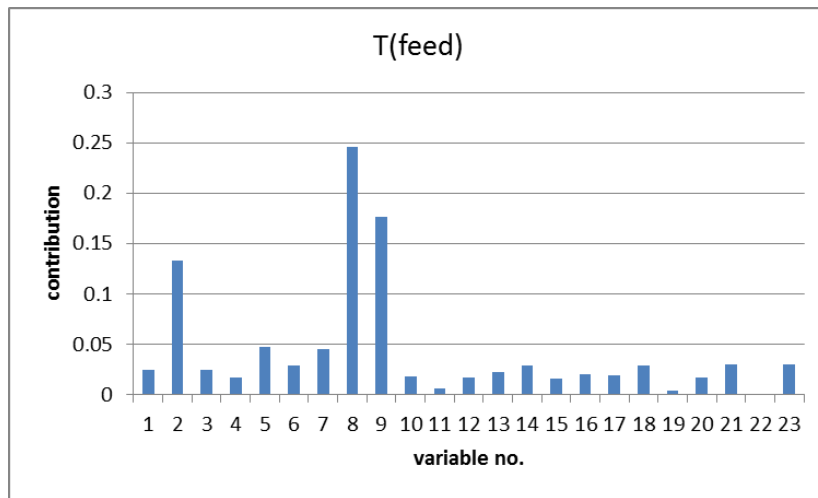
For example, in this faulty scenario the contribution plots bring our attention to regenerator side and highlights four suspected variables in that area. The causality analysis sketches the causality between those suspected variables to find the root cause. The values of transfer entropy approve the network that has been developed by Granger causality (Fig. 3.7a). Based on this network ambient air temperature affects the other three variables while it is not affected by other variables that indicates that ambient temperature is the root cause for this abnormal event. Although the highest contribution from KPCA was for combustion air discharge pressure, but the simplified causality network shows that among these variables ambient temperature has the ability to effect the other variables. This simplified causality network is also consistent with the original network developed based on all 23 variables. However, it is simpler and clearer in describing the causality between variables.



(a)



(b)



(c)

Figure 3.6. KPCA results for FCC (a) T^2 Hotelling. Contribution plots for (b) fault in ambient temperature (c) fault in fresh feed temperature

Second abnormal event: The second faulty scenario begins with normal operation for 1000 seconds and then is followed by a 10°C increase in fresh feed temperature for the remaining 4000 seconds.

In detection phase of the proposed method, the KPCA model construction is the same as first faulty case. The Hotelling T^2 and contribution plots of the KPCA analysis are shown on the Fig. 3.6. On Fig. 3.6a, the Hotelling T^2 values exceed the threshold after fault initiated indicating a successful detection of the mentioned fault. As can be seen in Fig. 3.6a, there is a small delay associated with the detection phase; however the lag time is smaller than that of the first abnormal event. The reason is that increase in fresh feed temperature entering to the process will affect the process earlier than the case there is an increase in air temperature because more enthalpy will be entered to the process when the feed temperature increases rather than increase in air temperature. Fig. 3.6c shows contributions to occurrence of the fault. Based on this figure, the following variables have significant contribution to process deviation from steady state when there is a variation on fresh feed temperature:

- Fresh feed temperature
- Furnace temperature
- Preheated feed temperature
- Regenerator pressure
- Differential pressure.

Selection of these variables from contribution plots bring the attention mainly to the furnace, the bottom of the reactor, and the pressure in the system. In the fault diagnosis phase, the causality analysis will show the causal effect among variables in the suspected area selected by KPCA analysis. Table 3.6b, shows the results of Granger analysis on this abnormal event. The first row

of this table shows that fresh feed temperature has effect on furnace temperature and preheated feed temperature which in entering to riser. Also furnace temperature has influence on preheated feed temperature. In the third row, a variation on temperature of the feed entering to the reactor riser will affect both the differential pressure and the regenerator pressure. The fourth row indicates that regenerator pressure also has influence on differential pressure between reactor and regenerator. The mutual transfer entropy values for this abnormal condition are given in Table 3.7b. These results are in accordance with the results of Granger causality which all verify the causal effect elicited from process knowledge (Fig. 3.7b). Based on process knowledge, heat balance around furnace in steady state shows that the enthalpy of the preheated fresh feed temperature is equal to the enthalpy of fresh feed entering to the furnace plus the net amount of enthalpy given to the fresh feed by the furnace. At constant pressure in the furnace, the enthalpy is a function of temperature and consequently the preheated feed temperature (T_2) is affected by fresh feed entering to the furnace (T_1) and furnace temperature (T_3). Also any variation in solid material temperature entering to the reactor will increase the enthalpy content in the reactor and this will affect the pressure of the unit. Fig. 3.7b shows the constructed network based on both methods of causality analysis. Based on this network, fresh feed temperature has influence on the other variables, either directly or indirectly, while it cannot be affected by other variables indicating that this variable is qualitatively suspected to be the root cause of the abnormal variation in the process.

Table 3.6. Granger test results of variables in FCC unit. (a) Fault in ambient air temperature, (b) fault in fresh feed temperature

	T_{amb}	P_6	P_2	$F_{sucn,comb}$	
T_{amb}	-	66.65	3229.33	4554.66	Chi-sq
	-	0.0000	0.0000	0.0000	Prob.
P_6	0.8719	-	0.4768	1.09	Chi-sq
	0.6466	-	0.7879	0.5789	Prob.
P_2	0.8940	0.3213	-	73.76	Chi-sq
	0.6395	0.8516	-	0.4053	Prob.
$F_{sucn,comb}$	0.1874	0.0941	261.64	-	Chi-sq
	0.9105	0.9540	0.0000	-	Prob.

(a)

	T_1	T_3	T_2	P_6	ΔP_{RR}	
T_1	-	3536.90	62441.16	8733.5	12344.3	Chi-sq
	-	0.0081	0.0000	0.0843	0.0763	Prob.
T_3	4.8931	-	399.07	7844.4	14938.3	Chi-sq
	0.0866	-	0.0000	0.1023	0.06943	Prob.
T_2	3.9197	2.1850	-	89453	45433.4	Chi-sq
	0.1409	0.3354	-	0.0000	0.0343	Prob.
P_6	1232.554	45.544	564.433	-	97546.6	Chi-sq
	0.76534	0.75564	0.8874	-	0.0000	Prob.
ΔP_{RR}	34.543	7544.64	9844.4	3754.66	-	Chi-sq
	0.98576	0.4643	0.3453	0.64665	-	Prob.

(b)

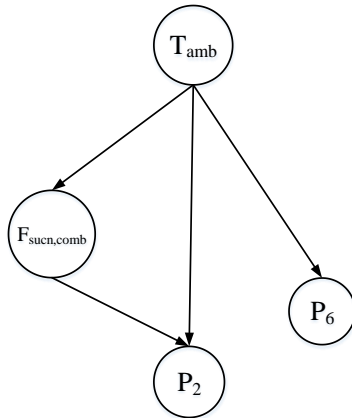
Table 3. 7. Transfer entropy between the most effective variables in two fault scenarios (a) fault in ambient temperature (b) fault in fresh feed temperature

	T_{amb}	P_6	P_2	$F_{sucn,comb}$
T_{amb}	-	0.13	0.27	0.23
P_6	-	-	<0.1	<0.1
P_2	-	-	-	-0.25

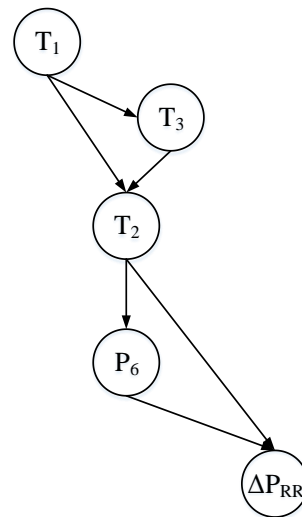
(a)

	T_1	T_3	T_2	P_6	ΔP_{RR}
T_1	-	0.24	0.38	<0.1	<0.1
T_3	-	-	0.42	<0.1	<0.1
T_2	-	-	-	0.34	0.65
P_6	-	-	-	-	0.16

(b)



(a)



(b)

Figure 3.7. Causal network of two faulty scenario in FCC (a) fault on ambient temperature (b) fault on fresh feed temperature

3.3.2. Tennessee Eastman Chemical Process

In order to further demonstrate the performance of the proposed method, it was applied to diagnose some faults in Tennessee Eastman Chemical process. This process consists of five major units: a reactor, condenser, compressor, separator, and a stripper; and, it contains eight components: A, B, C, D, E, F, G, and H. The process flow diagram of this process is shown in Fig. 3.8. It consists of 41 measured variables and 12 manipulated variables. Among measured variables, 22 variables are continuous process variables and 19 variables are related to composition measurements. The 22 continuous process variables are shown in Table 3.8 that are the main focus of this research. There are 21 faults in this process but among them we concentrate our study on those that are mentioned in Table 3.9 [3].

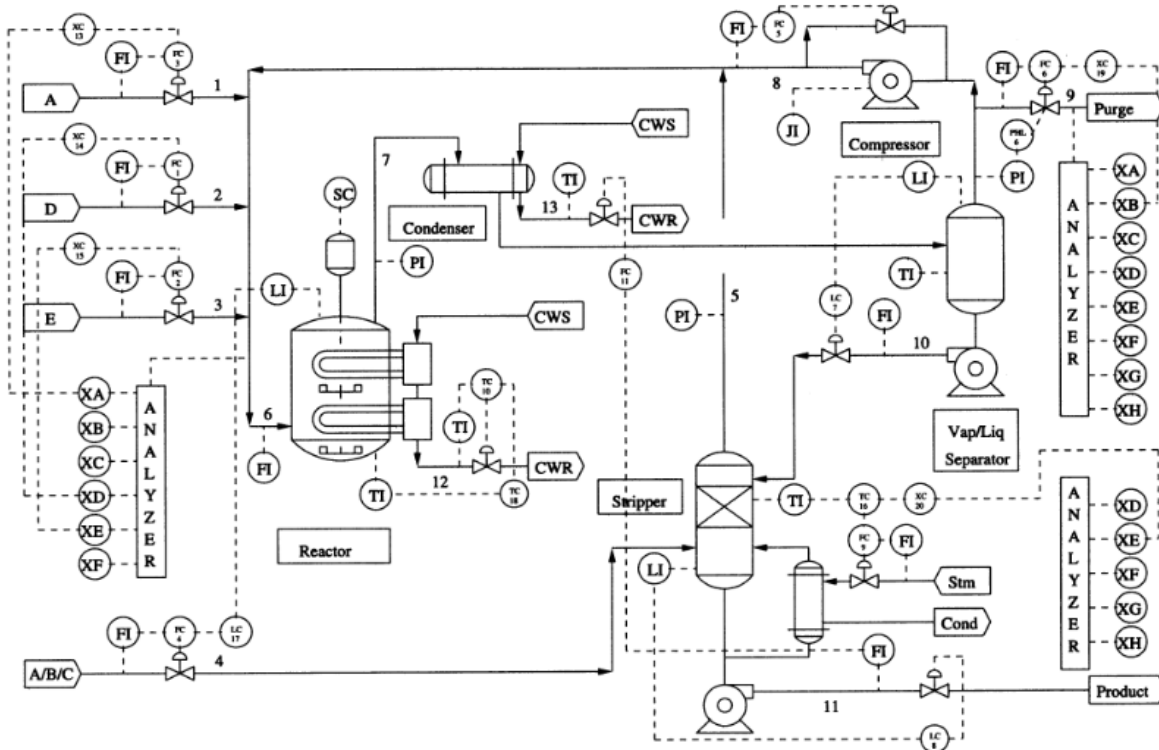


Figure 3.8. Schematic of Tennessee Eastman process

Table 3.8. Measured variables in TE

Variable	Description
XMEAS(1)	A feed (stream 1)
XMEAS(2)	D feed (Stream2)
XMEAS(3)	E feed (Stream 3)
XMEAS(4)	Total feed (Stream 4)
XMEAS(5)	Recycle flow (Stream 8)
XMEAS(6)	Reactor feed rate (Stream6)
XMEAS(7)	Reactor pressure
XMEAS(8)	Reactor level
XMEAS(9)	Reactor temperature
XMEAS(10)	Purge rate (Stream 9)
XMEAS(11)	Separator temperature
XMEAS(12)	Separator level
XMEAS(13)	Separator pressure
XMEAS(14)	Separator underflow (Stream 10)
XMEAS(15)	Stripper level
XMEAS(16)	Stripper pressure
XMEAS(17)	Stripper underflow (Stream 11)
XMEAS(18)	Stripper temperature
XMEAS(19)	Stripper steam flow
XMEAS(20)	Compressor work
XMEAS(21)	Reactor Cooling Water Outlet temperature
XMEAS(22)	Separator cooling water outlet temperature

Table 3. 9. Fault scenarios in TE

Fault no.	Fault description
IDV(6)	A step in feed loss in A
IDV(12)	A random variation in condenser cooling water inlet temperature

First abnormal event: The first faulty scenario is related to a normal operation for 500 seconds and a loss in A feed for remaining 500 seconds. This variation will affect the concentration of all components in the reactor. Consequently, this may change the process parameters in reactor and downstream units.

Based on KPCA performance on these scenarios the T^2 statistic was equal to 21.5 that is obtained based on confidence level of 0.95 and selection of four principal components, which show 85% of the variation in the system. Gaussian kernel function was selected in data analysis. As it is obvious in Fig. 3.9a there is a sharp jump in Hotelling T^2 values and they exceed the threshold instantaneously when the abnormality initiated indicating that KPCA is able to detect the A feed loss quickly. The contribution plot of this scenario is also given in Fig. 3.9b. In this abnormal event the following variables have high contribution among other variables:

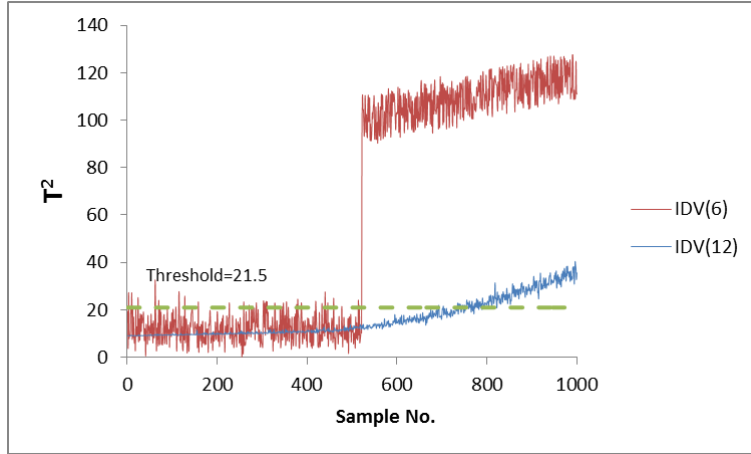
- XMEAS(1): A feed
- XMEAS(7): reactor pressure
- XMEAS(9): reactor temperature
- XMEAS(10): purge rate

- XMEAS(20): compressor work
- XMEAS(21): reactor cooling water outlet temperature

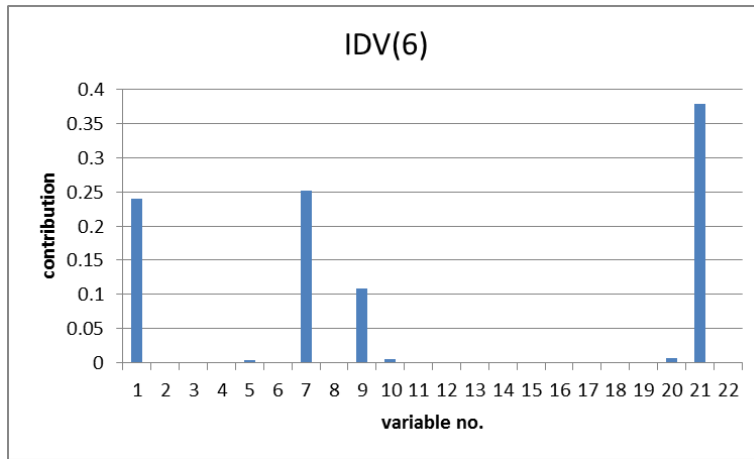
This indicates that a loss in A feed will affect the reactor and the compressor and the upstream of the separator that seems reasonable from process point of view. The reactants in this process are gaseous and a drop in the flow rate of one of these reactants will affect the pressure of the reactor. Also a loss in A feed concentration will deviate the kinetic of the reaction in the reactor since there is an exothermic reaction in the reactor and it may lead to variation in reactor temperature. Consequently the outcome of reactor will be different of normal outcome and this will affect the downstream units. It should be noted that the reactant A will be stripped in the stripper and the downstream product of stripper does not contain the reactant A. It is obvious that a loss in A feed will affect the composition of the final downstream product. However, since this paper did not take into account the composition of different materials as variables and only considered the process variables, in contribution plot the parameters of stripper have not high value of contribution on abnormal process variation. Considering these variables, it is difficult to accurately find which variable is most suspected to be the true root cause of the fault. So it is substantial to now the cause and effect relation between variables involved in the process.

The causality analysis methods suffer from the complexity of calculation when too many variables are involved in the calculations. Also, implementation of causality analysis on all variables in the process will not have precise and reliable fault diagnostic results because when there are too many variables, the constructed network based on causality analysis will be too complex, busy and difficult to qualitatively determine the root cause of the fault (Fig. 3.1b). So causality analysis was performed on the variables selected through KPCA in order to have a less busy network which facilitates the aim of fault diagnosis. Based on the Granger causality test on the most contributed

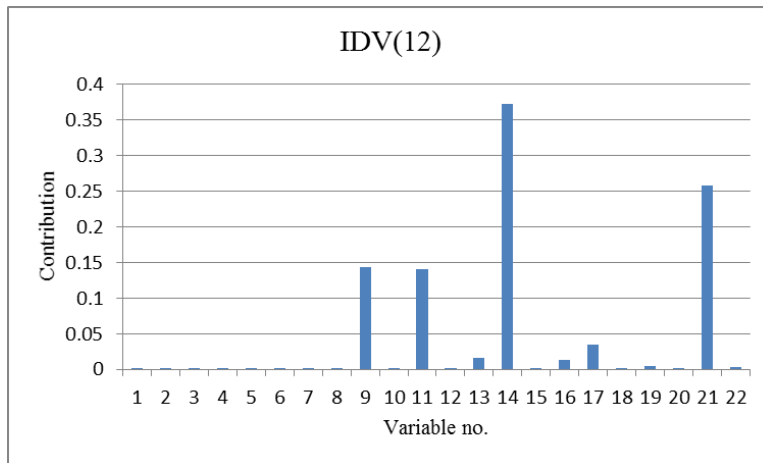
variables of this abnormal scenario (Table 3.10a) a simple networks will be constructed as in Fig. 3.10a. In this table the variables in first column are cause and the variables in the first row are effect variables. If the $prob < 0.05$, the variable in column has influence on the variable in row. For example $prob_{XMEAS(7) \rightarrow XMEAS(9)} = 0.0000$. It means XMEAS(7) which is reactor pressure has influence on XMEAS(9) which is reactor temperature. However, XMEAS(7), or reactor pressure, has not influence on XMEAS(1), which is A feed stream, because $prob_{XMEAS(7) \rightarrow XMEAS(1)} = 0.1093$. On the first faulty scenario and based on the first row of Table 3.10a, A feed stream has influence on reactor pressure. Based on second row, reactor pressure has influence on reactor temperature and based on the third row, reactor temperature has influence on purge rate, compressor work, and reactor cooling water outlet temperature. Based on this table one can construct a network containing six nodes and five arcs as it is shown in Fig. 3.10a. In order to further investigate the causal dependency between these nodes, the mutual transfer entropy values were computed for all pairs of this abnormal event (Table 3.11a). These results are in accordance with that of Granger causality and the constructed network based on transfer entropy is the same as Granger causality. As a result the constructed network based on causality analysis in all scenarios is sparse enough to guide us to find the root cause of the fault in the process. The proposed methodology finds A feed, XMEAS(1) as the main cause of fault since, according to figure 3.10a, this variable has influence on other variables while it is not affected by other variables.



(a)



(b)



(c)

Figure 3.9. KPCA results for Tennessee Eastman (a) T² Hotelling. Contribution plots for (b) IDV(6) (c) IDV(12)

Second abnormal event: The second fault is related to a normal operation of the process for 500 seconds and then the fault initiated with a random variation in condenser cooling water inlet temperature. This variable is not among measured variables. The source variables connected to this fault are in literatures [89].

Since the training data for both faulty scenarios in Tennessee Eastman are the same, the KPCA model construction for the second faulty scenario is the same as the first one. Figure 3.9a shows the departure of T^2 values beyond the threshold (threshold=21.5). Although the first faulty scenario that was a step variation in the process was detected abruptly, the detection of the second fault that is a kind of random variation in the process variable deals with a delay. The main reason is because the magnitude of the variation in condenser cooling water inlet temperature is less than the magnitude of the step in A feed flow rate. The contribution plot is given in Fig. 3.9c. The following variables have high contribution to this fault:

- XMEAS(9): reactor temperature
- XMEAS(11): separator temperature
- XMEAS(13): separator pressure
- XMEAS(14): separator underflow
- XMEAS(16): stripping pressure
- XMEAS(17): stripping underflow
- XMEAS(21) : reactor cooling water outlet temperature

Since this fault affects whole units of the process even the most downstream unit which is stripper, it seems that whole the process is under influence of this fault.

For the second abnormal event and based on the first row of Table 3.10b, reactor temperature has influence on both separator temperature and reactor cooling water outlet temperature. Bases on the second row, separator temperature has influence on separator pressure. The third row shows that the separator pressure affect the separator underflow and the forth row shows that separator underflow affects stripping pressure and stripping underflow. The constructed network is given on Fig. 3.10b. In order to further investigate the causal dependency between these nodes, the mutual transfer entropy values were computed for all pairs between variables selected by KPCA (Table 3.11). These results are in accordance with that of Granger causality and the constructed network based on transfer entropy is the same as Granger causality. As a result the constructed network based on causality analysis in all scenarios is sparse enough to guide us to find the root cause of the fault. For this faulty scenario, when there is a random variation in condenser cooling water inlet temperature, reactor temperature was accurately diagnosed as failure cause. Since there is no measurement in condenser cooling water inlet temperature, this method is able to find the variable that is mostly affected by the main root (XMEAS(9)) and is able to propagate the fault to other variables.

Table 3.10. Granger causality test for Tennessee Eastman process. (a) IDV6, (b) IDV12

	XMEAS(1)	XMEAS(7)	XMEAS(9)	XMEAS(10)	XMEAS(20)	XMEAS(21)	
XMEAS(1)	-	34654.89	833.43	184.83	8333.3	9034	Chi-sq
	-	0.0000	0.5422	0.634	0.234	0.2338	Prob.
XMEAS(7)	843.54	-	23856.23	4903.94	8473.5	232.43	Chi-sq
	0.1093	-	0.0000	0.2954	0.2393	0.5423	Prob.
XMEAS(9)	9433.34	5433.5	-	65921.45	32403.34	65332.5	Chi-sq
	0.5343	0.3433	-	0.0252	0.0000	0.0000	Prob.
XMEAS(10)	465.54	845.64	8394.4	-	938.53	9545.4	Chi-sq
	0.6743	0.5323	0.09842	-	0.7643	0.1235	Prob.
XMEAS(20)	9034.3	584.43	129.64	7845.54	-	834.34	Chi-sq
	0.4354	0.5434	0.76483	0.3435	-	0.1334	Prob.
XMEAS(21)	14924.4	9453.45	49334.34	4544.24	233.34	-	Chi-sq
	0.0754	0.3234	0.06343	0.3434	0.74453	-	Prob.

(a)

	XMEAS(9)	XMEAS(11)	XMEAS(13)	XMEAS(14)	XMEAS(16)	XMEAS(17)	XMEAS(21)	
XMEAS(9)	-	4323.23	20394.23	232.32	3498.343	83439.34	34782.23	Chi-sq
	-	0.0000	0.32932	0.3343	0.23543	0.5343	0.0000	Prob.
XMEAS(11)	89.5343	-	98343	89.34	89394.3	3534.34	949.33	Chi-sq
	0.6745	-	0.0000	0.4343	0.3434	0.07644	0.5343	Prob.
XMEAS(13)	8634.3	1244.44	-	6444.3	9543.3	53433.3	4343.23	Chi-sq
	0.64553	0.3352	-	0.0000	0.3353	0.5333	0.09443	Prob.
XMEAS(14)	8349.3	789.98	4578.7	-	58909.09	9579.87	8906.8	Chi-sq
	0.0934	0.7866	0.3447	-	0.0000	0.0000	0.1009	Prob.
XMEAS(16)	9324.43	7343.343	8343.22	39083.34	-	4434.44	66.97	Chi-sq
	0.5453	0.5434	0.2232	0.4334	-	0.5433	0.6997	Prob.
XMEAS(17)	9384.34	834.33	8422.2	7278.254	1222.22	-	8732.2	Chi-sq
	0.4534	0.4332	0.4222	0.9873	0.3222	-	0.2433	Prob.
XMEAS(21)	76304.3	1.4323	52.432	9722.33	97622.2	655.33	-	Chi-sq
	0.54347	0.8837	0.4382	0.75222	0.0683	0.8722	-	Prob.

(b)

Table 3.11. Transfer entropy between the most effective variables in two faulty scenarios in Tennessee Eastman (a) IDV6, (b) IDV12

	XMEAS(1)	XMEAS(7)	XMEAS(9)	XMEAS(10)	XMEAS(20)	XMEAS(21)
XMEAS(1)	-	0.22	<0.1	<0.1	<0.1	<0.1
XMEAS(7)	-	-	0.43	<0.1	<0.1	<0.1
XMEAS(9)	-	-	-	0.45	0.32	0.23
XMEAS(10)	-	-	-	-	<0.1	<0.1
XMEAS(20)	-	-	-	-	-	<0.1
XMEAS(21)	-	-	-	-	-	-

(a)

	XMEAS(9)	XMEAS(11)	XMEAS(13)	XMEAS(14)	XMEAS(16)	XMEAS(17)	XMEAS(21)
XMEAS(9)	-	0.23	<0.1	<0.1	<0.1	<0.1	0.55
XMEAS(11)	-	-	0.43	<0.1	<0.1	<0.1	<0.1
XMEAS(13)	-	-	-	0.19	<0.1	<0.1	<0.1
XMEAS(14)	-	-	-	-	0.53	0.48	<0.1
XMEAS(16)	-	-	-	-	-	<0.1	<0.1
XMEAS(17)	-	-	-	-	-	-	<0.1
XMEAS(21)	-	-	-	-	-	-	-

(b)

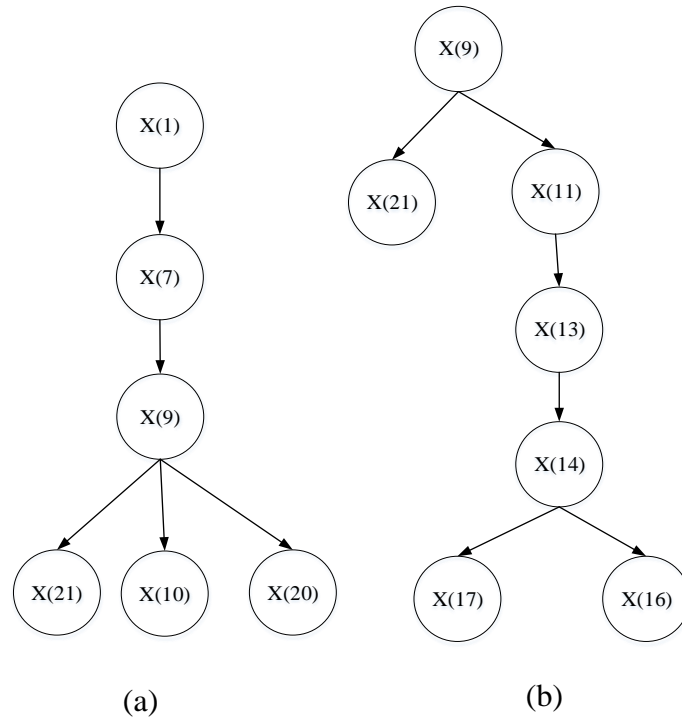


Figure 3.10. Constructed networks based on proposed technique for Tennessee Eastman process. (a) IDV6, (b) IDV12

3.4. Conclusion

Although KPCA is a powerful tool in multivariate analysis for detection and even in identification of faults, it suffers in linking the fault to its root cause. In case of an abnormality on an industrial process, it is difficult for an operator to have an accurate diagnosis of the root cause of a fault based on the contribution plots in KPCA analysis. Besides, contribution plots may contain spurious contributions that are related to noise in the process variables. In such a case, combining KPCA with another method is worthwhile. Here it was shown that KPCA combined with causality analysis is an appropriate tool for process fault detection and diagnosis. The importance of this methodology is due to providing a visual cause and effect description among the variables that are most suspected to be the root cause of the fault. The proposed methodology was applied to FCC and Tennessee Eastman Chemical process. In both examples KPCA was able to detect the fault but could not diagnose the main cause of fault. Based on network construction, causality analysis diagnosed the root cause of the fault and showed the propagations pathway of the fault to other affected variables. Also in both examples, causality analysis was done by both transfer entropy and granger causality test and comparison between them verifies the previous theories in this area: when the process variables have Gaussian, exponential Weibman, or log-normal data distribution, Granger causality has the same result as transfer entropy which represents the amount of information that transfers from one variable to other neighbor or non-neighbor variable.[75, 76].

Chapter 4

Root cause diagnosis of process fault using KPCA and Bayesian network

Abstract: This paper develops a methodology to combine diagnostic information from various fault detection and isolation tools to diagnose the true root cause of an abnormal event in industrial processes. Limited diagnostic information from kernel principal component analysis (KPCA), other on-line fault detection and diagnostic tools, and process knowledge were combined through Bayesian belief network (BBN). The proposed methodology will enable an operator to diagnose the root cause of the abnormality. Further, some challenge on application of Bayesian network on process fault diagnosis such as network connection determination, estimation of conditional probabilities, and cyclic loop handling were addressed. The proposed methodology was applied to Fluid Catalytic Cracking unit and Tennessee Eastman Chemical Process. In both cases, the proposed approach showed a good capability of diagnosing root cause of abnormal condition.

4.1. Introduction

In process industries, there has been a continuing demand for higher quality products and lower product rejection rates, satisfying increasingly stringent safety and environmental regulations [1]. Implementation and improvement of accurate control scheme have been essential over the recent decades in order to meet these ever increasing standards [90]. Modern control systems became

extremely complex by integrating various functions and components for sophisticated performance requirement [3, 40]. With such complexities in hardware and software, it is natural that the system may become vulnerable to faults in practice and fault diagnostic tools are required to ensure the process safety and quality of products. The objectives of these tools are early detection of faults and to minimize the impact of a fault on the system [3].

In the recent years extensive research has been conducted on process fault detection and diagnosis (FDD). According to the comprehensive review of Venkatasubramanian et al., FDD tools can be divided to model-based methods and process history based methods [4, 10, 23]. Model based methods require precise mathematical relationship between internal states of the process. Most of the times is impossible to have such a precise model [14, 91]. History based methods uses the data of the process that contain all normal and abnormal condition in the process and implement these data for training and fault detection purpose [92]. Although these methods are effective to detect faults early and widely used in process industries, the diagnosis of the faults is not precise. Various residual evaluation methods have been developed to uniquely identify the fault location, for example, generalized likelihood ratio test [15], and structured residuals [93]. However, the inaccuracy in fault diagnosis still exists and often these methods point towards response variables as the root cause.

In order to overcome the limitations of individual methods and improve the diagnose ability of process faults, hybrid methods have been proposed by researches in recent years. A hybrid framework consists of collection of methods and utilizes information from several FDDs to overcome the limitations of individual methods [5-7]. This combination of different methods allows one to evaluate different kinds of knowledge in one single framework for better decision making [7]. For instance, the analytical methods in model-based fault detection and diagnosis are

based on residual generation using parameter estimation; however, the robustness of the model-based methods is often under question since obtaining an accurate model for process, especially for chemical processes, is challenging. To address this problem, Frank proposed the use of analytical methods and integrated them with knowledge-based methods. He combined the analytical methods with expert system approach which makes use of qualitative models based on available information of the process, facts and rules. Degree of ageing, used tools and history of operation are examples of expert knowledge. They concluded that knowledge-based methods complement the shortcomings of analytical methods of fault diagnosis [16]. An integration of neural network and expert system for fault diagnosis was done by Becraft et al. Once the process fault was localized by neural network, the results were analyzed by a deep knowledge expert system including information of the system structure, function and principles of operation [64]. Mylaraswamy provided a brief comparison of the various diagnostic methods to highlight the inadequacy of individual methods and underscored the need for collective problem solving. They proposed a Dkit based hybrid method of neural network for detection of a fault and a SDG for diagnostic action [6]. Zhao et al. proposed a wavelet-sigmoid basis neural network for dynamic diagnosis of failure in hydrocracking process [5].

Process measurements are very noisy and there is uncertainty in the relationship between process variables. A BN model is an excellent tool to characterize processes with stochastic uncertainty using conditional probability-based state transitions [57]. Hence, it can be adopted to identify the propagating probabilities among different measurement variables so as to determine the operating status of processes and diagnose the root causes of abnormal events [56]. Researchers have used BN for improving process fault diagnosis in different ways. Due to stochastic nature of process variation, a false alarm may be generated in monitoring system while the process is operating in

normal condition. To address this problem, in the methodology proposed by Dey et al., data from multiple sensors were combined through a causal belief network to estimate probabilistic diagnosis of root cause of the process fault. They showed that the posterior probability of each node which shows the status of the node can be updated from evidence using Pearl message passing algorithm [56]. Yu et. al proposed a Bayesian inference-based abnormality likelihood index to detect a process fault. In diagnosis phase they utilized dynamic Bayesian probability and contribution indices [57]. In complex processes, it is not economic to monitor all the variables while sometimes fault is originated in the non-monitored variables. To address this issue, Yu et al. investigated the possibility of combining modified ICA and BN for process FDD. The limited diagnostic results of ICA was used as evidence in BN updating and concluded that the combined framework of these two methods is a strong tool for FDD purpose for all monitored and non-monitored variables [36]. Despite these researches, there is still more need to research in this area especially since it is somewhat unclear how to use the outcome of data-based FDD methods as an input to the knowledge based root cause analysis in an automated fashion. Also in these researches, the causal relationships in the network were determined using process knowledge and conditional probabilities are assigned based on expert judgement which is subjective as it heavily depends on the knowledge and experience of individuals. Furthermore, there is ambiguity in whether one should use normal or faulty data for network training and details on preprocessing of training data is not discussed [36, 57]. Some application challenges arise due to the inherent limitations of Bayesian network. A BN in its original form is an acyclic directed graph. In chemical processes, however, cyclic loops appear due to material and heat integration; recycle streams, as well as information flow paths due to feedback control. As such, BNs needs to be adopted to represent chemical processes adequately.

Our research aims to fill these knowledge gaps with view to developing a comprehensive methods that can precisely diagnose the root cause of process fault and help the operator to take corrective actions. We propose a new methodology through integration of diagnostic information from various single variable and multivariable diagnostic tools using BN. We also address the application difficulties of BN related to process fault diagnosis. We used Granger causality and transfer entropy to determine the causal relationships between process variables. A detailed methodology for estimating conditional probabilities between variables is also proposed in this paper. Cyclic networks were dealt with through transformation of cyclic BN to acyclic-BN using pseudo-nodes. We demonstrated the efficacy of the proposed methodology through two case studies, i.e. FCC and Tennessee Eastman.

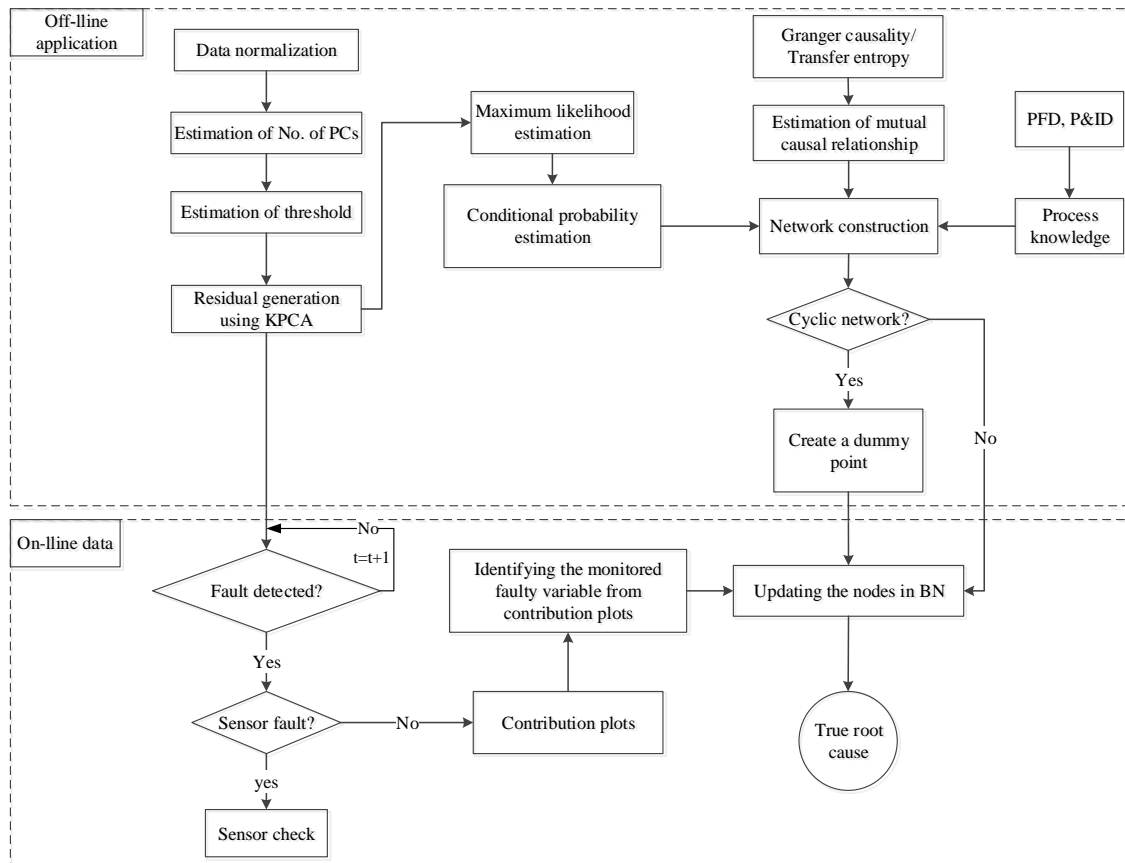


Figure 4.1. The proposed method for root cause diagnosis of process fault

4.2. Methodology: BN-based process monitoring approach

The overall picture of the methodology is given in Fig. 4.1. The main components of the proposed methodology are: KPCA model, sensor fault detection module, and BN. In an on-line setting KPCA will act as a primary tool for detecting process fault. Having detected the fault, next step would be to diagnose the root cause of the fault and the propagation pathway. The fault may be originated among internal states or it may be because of a sensor malfunction. It is important to isolate sensor faults using sensor validation module since these kind of faults breakdown the correlation between variables and the causality networks do not work effectively. A sensor check module can be designed using simple rule-based algorithms or more sophisticated algorithms such as bank of Kalman filter with weighted sum of squared residual (WSSR) [94]. To keep the methodology simple, we used a rule-based algorithm. If the sensors are working properly, the failure should be among process internal states. The BN is more appropriate to detect disturbance type faults. Thus, if it is a sensor fault the algorithm stops at this point. Otherwise it will proceed to determining the root cause of the fault. The average contributions calculated from the KPCA is used to preliminarily diagnose the causes of faults. This information is passed on to the trained BN as evidence. The trained BN based on its causal relations and conditional probabilities determine the true root cause of the fault. The training of the KPCA and BN is done in an off-line mode. Important steps in building a KPCA model are data normalization, determining the number of PCs, residual generation using training data set.

BN has two components: construction of causal network and estimating the conditional probabilities. Granger causality and transfer entropy was applied for estimation of mutual causal relationship between variables and for construction of network. Knowledge of the process was used to verify the constructed network. If the network contained a loop, a dummy duplicate node

was created for one of the variables involved in the loop because Bayesian network cannot update cycles. Conditional probabilities among different nodes are the quantitative part of the network which was calculated using maximum likelihood method. Our objective was to reflect the causal relationships among the variables due to abnormal events as such we used the residuals from the KPCA to calculate the conditional probabilities. The residuals contain only the abnormal process variations thus conditional probabilities calculated from the residuals better reflect the propagation pathways of the faults. More detail on each section is presented in following sections:

4.2.1. Kernel Principal Component analysis (KPCA)

KPCA is an extension of PCA to deal with nonlinear data set. In KPCA, nonlinear data can be converted to linear form through high-dimensional mapping. For example, a data set x and z which are not separable in current space are linearly separable in nonlinear hyperplane with features $\Phi_i(x)$ and $\Phi_j(z)$. Thus KPCA is a two-step method: calculation of covariance matrix and dot products of variables in feature space, and singular value decomposition of covariance matrix in feature space. Finding the exact feature space is not straight forward and calculation of the dot products in the feature space can be prohibitive due to calculation complexities. Instead of explicitly transforming variables to feature space, dot product vectors in feature space is calculated using Kernel function. According to [87] the dot product of the transformed variables is given by the following equation:

$$k(x, z) = \Phi_i(x) \cdot \Phi_j(z) \quad (4.1)$$

The function $k(\cdot, \cdot)$ is called the kernel function, and there exist several types of these functions. Some popular kernel functions are polynomial functions, Gaussian functions, and sigmoidal functions [28, 32]. The fault detection in KPCA is done using Hotelling T^2 which is similar to PCA. The contributions of each variable reflect some useful information in diagnosis. However,

unlike PCA contribution of KPCA model cannot be calculated easily because of the nonlinear transformation in KPCA. Alcalá and Qin proposed reconstruction-based contribution (RBC) to overcome the aforementioned shortcoming and to estimate contribution of each variable [87, 88]. The procedure to estimate fault free data by eliminating the effect of fault from faulty data is defined as reconstruction.

$$z_i = x_i - \xi_i f_i \quad (4.2)$$

where z_i is fault free data, x_i is faulty data, ξ_i is the direction of fault, and f_i is the magnitude of fault. RBC considers the reconstruction of a fault detection index (T^2 or SPE) along the direction of a variable as the variable's contribution for that fault. In other words, the objective of RBC is to find f_i of a vector with direction ξ_i such that the fault detection index of the reconstructed measurement is minimized. The reason for minimization is that for fault free data the detection index should be minimum; however it is not zero because there is always some process normal variation and noise in a process.

The residuals from the KPCA module were used to update the probability of the corresponding nodes in the BN. The residual components are calculated from:

$$\tilde{t} = P_f^T \Phi \quad (4.3)$$

Where P_f^T is related eigenvectors corresponding to remained PCs which are related to residuals and Φ is the mapped vector of observation space. The calculation of residual from equation 4.3 is not possible because of high dimensionality in feature space. Here we calculated residuals from the difference between faulty data and fault free data which is obtained from reconstruction:

$$e_i = x_i - z_i \quad (4.4)$$

More details and the mathematics behind the theory is given in Appendix.

4.2.2. Sensor failure module

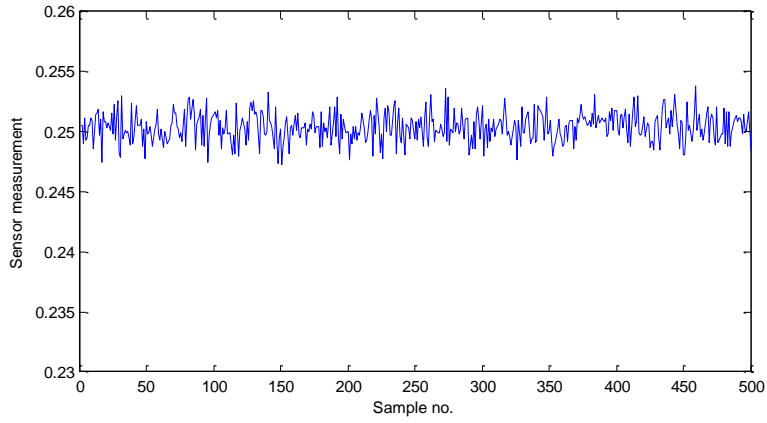
In the proposed method, a rule-based sensor check module has been designed after KPCA unit to isolate sensor malfunction. According to Sharma et al. the following failures are probable in a sensor [95]:

- **FLAT LINE:** The sensor reports a constant value for a large number of successive samples (Fig. 4.2b).
- **SPIKE:** A sharp change in the measured value between two successive data points (Fig. 4.2c).
- **NOISE:** The variance of the sensor readings increases. Unlike SPIKE faults that affect a single sample at a time, NOISE faults affect a number of successive samples (Fig. 4.2d).

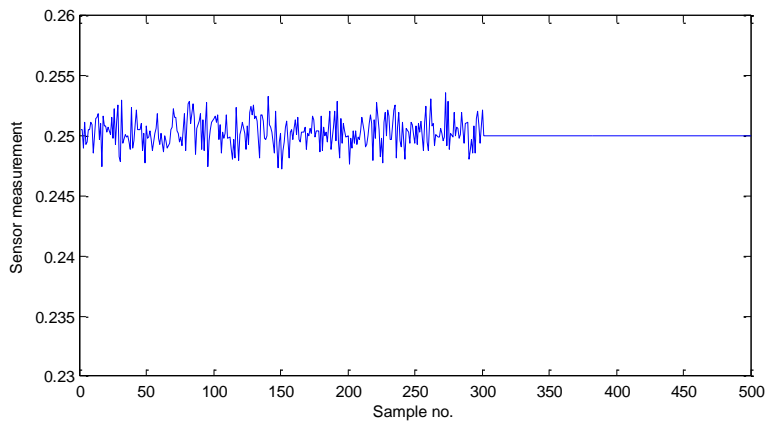
In order to keep things simple we used the following rules to detect these faults:

- When the difference between two consecutive observations is less than a very small value and this happens for five consecutive observations, the sensor is suspected to Flat line failure.
- When the difference between two consecutive observations is a very large number in comparison with the standard deviation of data, the sensor is suspected to Spike failure.
- If in any data window of N data points, q measured values of a sensor exceed the threshold, the sensor is suspected for Noise failure.

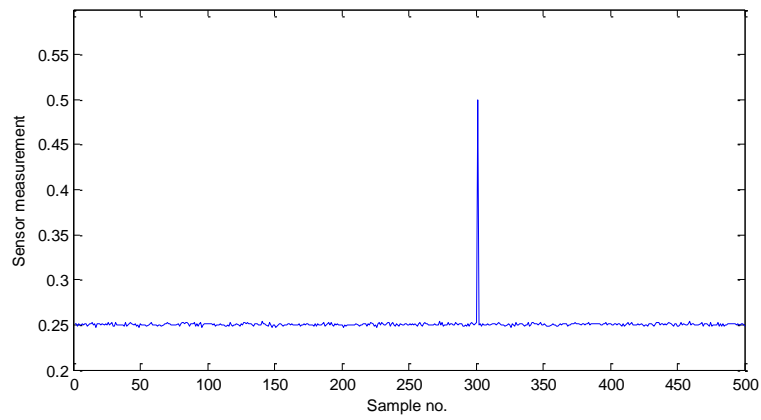
Pseudo-code to apply the above heuristics is given in Fig. 4.3.



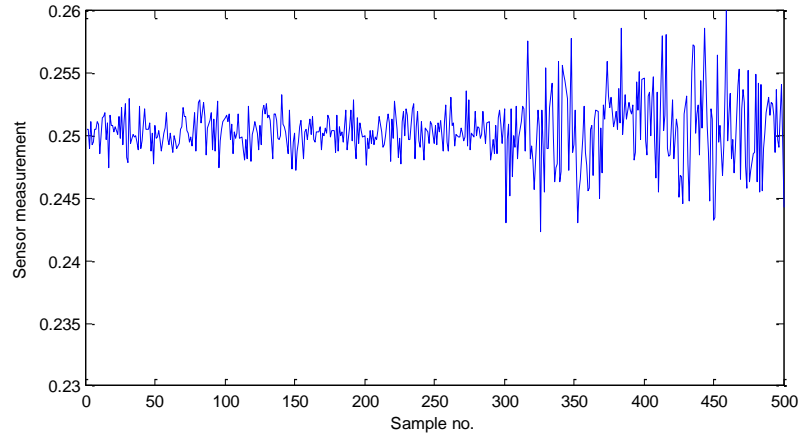
(a)



(b)



(c)



(d)

Figure 4.2. Normal and faulty states of a sensor (a) Normal performance (b) flat line fault (c) spike fault (d) noise fault

```

1.   Input
Data- a m*n matrix (m: observations, n: variables)
2.   Output: a diagnosis report
3.   For each sensor  $s_i \in n$ 
4.       If  $\text{Data}(p+1, i) - \text{Data}(p, i) < \epsilon \dots$  (for five consecutive observations)
5.           Break
6.           Sensor  $\rightarrow$  suspected
7.       If  $\max(\text{or min}) - \text{mean} \gg \text{st.dev}$ 
8.           Break
9.           Sensor  $\rightarrow$  suspected
10.  If  $\text{abs}(m \text{ values} - \text{mean}) > \text{threshold}$  for q samples a in window size N (N and q < m)
11.     Break
12.     sensor  $\rightarrow$  suspected
13.  if suspected
        report  $\rightarrow$  sensor fault diagnosed

```

Figure 4.3. Pseudo-code for sensor fault detection

4.2.3. Bayesian network construction

A BN is utilized to determine the fault origin and the pathway in which the fault is propagated. BN has two components: the causality network and conditional probabilities. Typically, in most cases the causal relationship and conditional probabilities are assigned based on process knowledge. In this study we show how to use process data to complement process knowledge. In order to construct the network, the mutual cause and effect relationship between variables should be determined. We employed Granger causality and transfer entropy to extract causal relationships among variables from process data. The detailed explanation on causality analysis and construction of the BN is described below:

4.2.3.1. Causality analysis based on Granger Causality

Wiener introduced the concept of history based causality, and later in 1969 Granger formulated it to show the cause and effect relationship among different variables in any system [69, 81]. According to Granger, a variable 'y' Granger causes the other variable 'x' if incorporating the past values of 'x' and 'y' helps to better predict the future of 'x' than incorporating the past values of 'x' alone [69]. Considering two time series x and y , there are two different linear regression model. One is a restricted model in which the prediction of x at time k is possible using the information of the past values of x :

$$x_k = \sum_{i=1}^p \mu_i x_{k-i} + \varepsilon_{xk} \quad (4.5)$$

where x_k is the value of x at time k ; x_{k-i} is the i -lagged value of x ; μ is the regression coefficient; p is the number of time lagged variables considered; and ε denotes the residual series for constructing x_k .

The second model is unrestricted model in which the prediction of x at time t is possible using the past information of both x and y as follows:

$$x_k = \sum_{i=1}^p \gamma_i x_{k-i} + \sum_{j=1}^q \beta_j y_{k-j} + \eta_{xk} \quad (4.6)$$

where x_k is the x time series at time k ; x_{k-i} and y_{k-j} are respectively the i -lagged x time series and j -lagged y time series; γ and β are the regression coefficients; p and q are the amount of lag considered or model order; and η denotes the unrestricted model residual at time k . The μ , β , and γ parameters are calculated using least squares method. A small value of p or q leads to poor model estimation while large values result in problem of overfitting. Akaike Information criterion (AIC) [82] and Bayesian Information criterion (BIC) [66] are two criteria that are used to determine the model order. AIC and BIC are given as follows:

$$AIC(p) = \ln(\det(\Sigma)) + \frac{2pn^2}{T} \quad (4.7)$$

$$BIC(p) = \ln(\det(\Sigma)) + \frac{\ln(T)pn^2}{T} \quad (4.8)$$

where Σ represents the noise covariance matrix and T is the total number of observations. When the variability of the residual of the unrestricted model is significantly reduced with that of a restricted model, then there is an improvement in the prediction of x due to y . In other words y is said to Granger cause x . This improvement can be measured by the F statistic:

$$F = \frac{(RSS_r - RSS_{ur})/q}{RSS_{ur}/(T-p-q-1)} \sim F(p, T-p-q-1) \quad (4.9)$$

where RSS_r is the sum of the squares of the restricted model residual, RSS_{ur} is the sum of the squares of unrestricted model residual, and T is the total number of observations used to estimate the model. F statistics approximately follows F distribution with degrees of freedom p and $(T-p-$

$q-1$). If the F statistics from y to x is significant, then the unrestricted model yields a better explanation of x than does the restricted model, and y is said to Granger cause x [84].

4.2.3.2. Causality analysis based on Transfer entropy

For two variables with sampling interval of τ , $\mathbf{x}_i = [x_i, x_{i-\tau}, \dots, x_{i-(k-1)\tau}]$ and $\mathbf{y}_i = [y_i, y_{i-\tau}, \dots, y_{i-(l-1)\tau}]$, information transferred from y to x is defined as follows [71]:

$$t(x|y) = \sum_{x_{i+h}, x_i, y_i} P(x_{i+h}, \mathbf{x}_i, \mathbf{y}_i) \cdot \log \frac{P(x_{i+h} | \mathbf{x}_i, \mathbf{y}_i)}{P(x_{i+h} | \mathbf{x}_i)} \quad (4.10)$$

where $P(\cdot)$ denotes the probability density function (PDF) and h is the prediction horizon. k and l show the length of time series. Transfer entropy represents the measure of information transfer from y to x by measuring the reduction of uncertainty while assuming predictability [71]. It is defined as the difference between the information about a future observation of x obtained from the simultaneous observation of past values of both x and y , and the information about the future of x using only past values of x . It was shown that the parameter values can be chosen as: $\tau = h \leq 4$, $k = 0$, and $l = 1$ for the initial trial [68]. Using the above definitions, direction and amount of net information transfer from y to x is as follows:

$$t(y \rightarrow x) = t(x|y) - t(y|x) \quad (4.11)$$

$t(y \rightarrow x)$ is causality measure and is derived by comparing the influence of y to x with influence of x to y . If $t(y \rightarrow x)$ is negative then information is transferred from x to y . Since at first there is no knowledge about which node is cause and which one is effect, choosing these nodes inversely will result in negative value.

The advantage of using transfer entropy is that it is a model free method and can be applied to non-linear data. It has already been proved to be very effective in capturing process topology and

process connectivity [96]. But it suffers from a large computational burden due to the calculation of the PDFs. Histograms or nonparametric methods, e.g. kernel method, can be used to estimate the PDF [71]. The Gaussian kernel function is used to estimate the PDF which is defined as follows:

$$K(v) = \frac{1}{\sqrt{2\pi}} e^{-\frac{1}{2}v^2} \quad (4.12)$$

Therefore, a univariate PDF can be estimated by,

$$p(x) = \frac{1}{N \cdot d} \sum_{i=1}^N K\left(\frac{x-x_i}{d}\right) \quad (4.13)$$

where N is the number of samples, d is the bandwidth chosen to minimize the error of estimated PDF. d is calculated by $d = c \cdot \sigma \cdot N^{0.2}$ where σ is variance and $c = (4/3)^{0.2} \approx 1.06$ according to the “normal reference rule-of-thumb” approach. For a q -dimensional multivariate case the estimated PDF is given by [71]:

$$P(x_1, x_2, \dots, x_q) = \frac{1}{N \cdot d_1 \dots d_q} \sum_{i=1}^N K\left(\frac{x_1-x_{i1}}{d_1}\right) \cdot K\left(\frac{x_q-x_{iq}}{d_q}\right) \quad (4.14)$$

where $d_s = c \cdot \sigma(x_{i,s})_{i=1}^N \cdot N^{-1/(4+q)}$ for $s = 1, \dots, q$.

4.2.3.3. Estimation of conditional probabilities

Besides the causal network, a BN contains conditional probability tables for all nodes. These values quantify the amount of influence each node receives from its parents. In this paper, calculation of conditional probabilities was done by maximum likelihood estimation (MLE). Suppose a sample consisting of m variables and n observations. We write $x_j^{(i)}$ for the j 'th observation of i 'th variable. Given these definitions, the MLE for $P(x)$ for $x \in \{1 \dots k\}$ takes the following form (k is the number of states):

$$P(x) = \frac{\sum_{j=1}^n [x_j^{(i)} = x]}{n} = \frac{count(x)}{n} \quad (4.15)$$

$[x^{(i)}=x]$ is 1 if $x^{(i)}=x$, otherwise it is equal to zero. Hence, $\sum_{i=1}^n [x^{(i)} = x] = count(x)$ is simply the number of times that the state x is seen in the training set, or number of times that state x is inside threshold that have been previously determined.

Similarly, the MLE for the $P(x | y)$, x and $y \in \{1 \dots k\}$, takes the following form:

$$P(x|y) = \frac{P(x,y)}{P(y)} = \frac{\sum_{j=1}^n [x_j^{(i)} = x \text{ and } y_j^{(i)} = y]}{\sum_{j=1}^n [y_j^{(i)} = y]} = \frac{count_j(x \text{ and } y)}{count(y)} \quad (4.16)$$

This is a very natural estimate and equal to the number of times state both x and y are seen within the threshold upon the number of times the label y is seen within the threshold [85].

In a process system, propagation path for fault and normal variation is often not the same [97]. The conditional probability in essence should reflect the causal relations between variables under faulty conditions. In order to keep only the variation of abnormality and noise and to mitigate the effect of process variation on the conditional probability calculation, the residuals from KPCA analysis were used for calculation of conditional probabilities (Fig. 4.6). Also the residuals follow Gaussian distribution more closely compared to the raw data, as such gives better maximum likelihood estimates. In other words, conversion of data to residuals will mitigate process variations in variable values while keeping the causality of fault information inside, consequently conditional probabilities estimated from residuals reflect the causal relations for faulty variables more accurately.

4.2.3.4. Construction of BN: An illustrative example

We will illustrate the network construction using Granger causality and transfer entropy and also estimation of conditional probabilities, for a simple dissolution tank system. [34]. In this system pure solid crystal is dissolved in a tank with water (Fig. 4.4). The flow of water to the tank is under control. Also the solid crystals are fed from a hopper to the tank through a rotary feeder. The control objective of this process is to maintain the level of water and concentration of crystal in the tank to desired set point. However, these two parameters are subjected to abnormal changes due to disturbance in the solid discharge.

There are four variables in this process, water flow to the tank, RPM of the rotary feeder, level of water, and concentration of solid crystal in the tank. These four variables are taken as nodes in a network and their values within the operation of the process will be analyzed by Granger causality and transfer entropy for network construction. We used a statistical software *Eviews* to perform Granger causality analysis. The results of Granger causality analysis are shown in Table 4.1. In this table based on the F statistics when the $prob < 0.05$, it rejects the null hypothesis and indicates the variable in the row has influence on the variable in column. For example, based on the first row of this table, water flow has influence on level and solid crystal concentration. Also the second row shows that the RPM has influence on level and solid crystal concentration as well. The network constructed based on this method is shown Fig. 4.5. Also we did causality analysis of the same system using transfer entropy. The results of transfer entropy are given in Table 4.2. In this model, there is time lag between inputs and outputs. In calculation of transfer entropy, several time delay values in the range of $[-5:5]$ were considered and the value with the maximum transfer entropy was selected. In Table 4.2, the value of transfer entropy indicates that the variables in rows have influence on the variables in columns. However, by comparison of the network

constructed by Granger causality and transfer entropy, there is a discrepancy in the results. Based on transfer entropy level of the tank has effect on solid crystal concentration; however, Granger causality does not confirm such a relation. The results of Granger causality are more accurate than that of transfer entropy because in calculation of conditional probability values of transfer entropy test, histograms were used that introduced some error to the calculation. In order to rectify the results, a threshold of 0.1 was set for transfer entropy values; only values above the threshold indicates that there is a significant causal relationship between the variables.

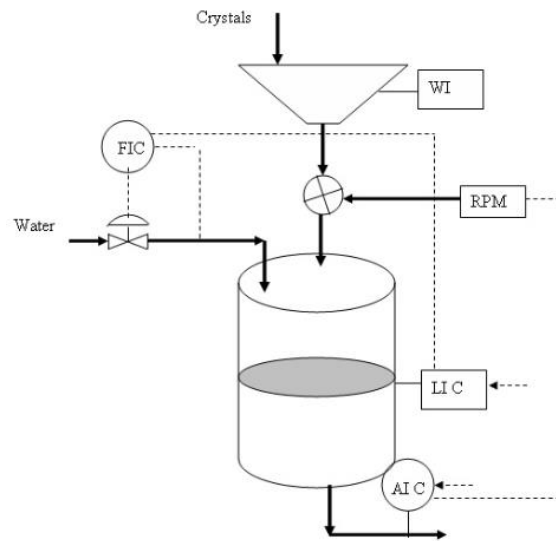


Figure 4.4. Process flow diagram of dissolution tank system

Table 4.1. The result of Granger causality analysis for dissolution tank system

	Water flow	RPM	Level	Concentration	
Water flow	-	66.65	53239.33	4554.66	Chi-sq
	-	0.1253	0.0000	0.0000	Prob.
RPM	0.7632	-	3424.43	76434.5	Chi-sq
	0.6466	-	0.0000	0.0000	Prob.
Level	53.332	0.7613	-	949.43	Chi-sq
	0.7524	0.0934	-	0.5322	Prob.
Concentration	13.644	6347.3	361.54	-	Chi-sq
	0.8323	0.0784	0.1125	-	Prob.

Table 4.2. Mutual transfer entropy values between nodes on dissolution tank system

	water in	Solid	level	concentration
water in	NA	NA	0.16	0.25
Solid	NA	NA	0.14	0.19
Level	NA	NA	NA	0.02

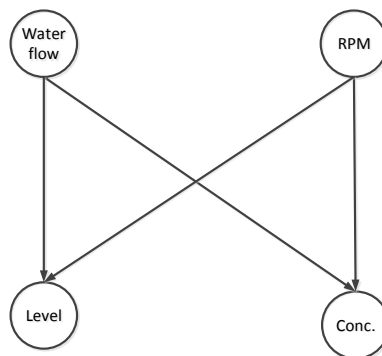
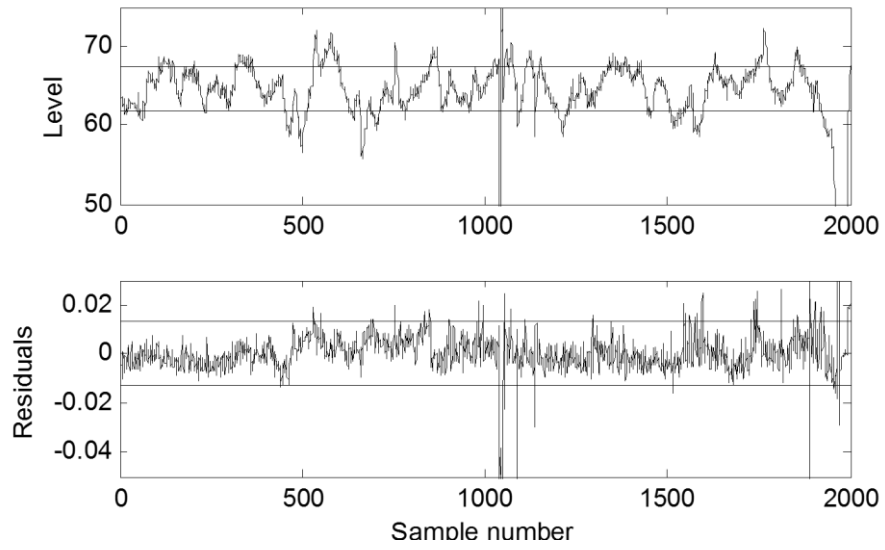
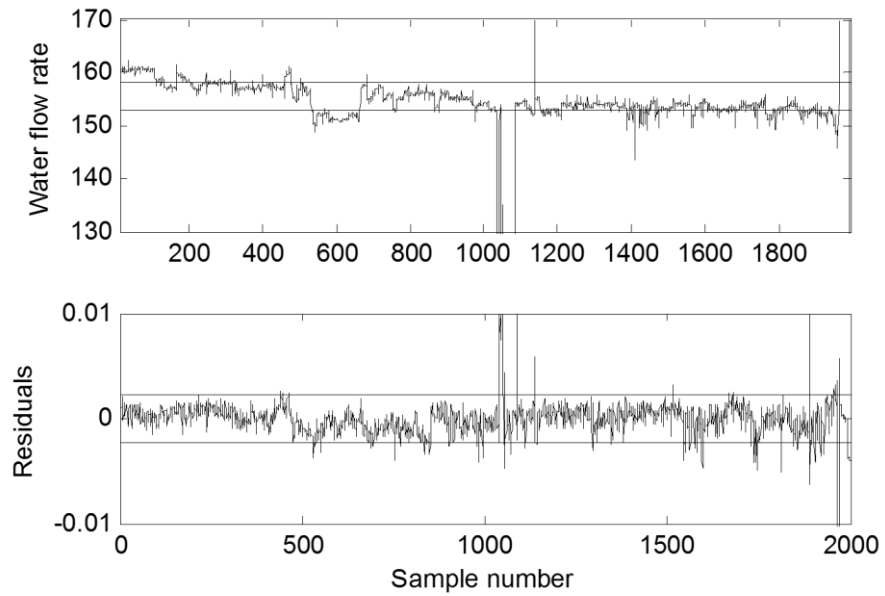


Figure 4.5. Constructed network for dissolution tank system using Granger causality and transfer entropy

Next we calculated the conditional probabilities for the system. Fig. 4.6 shows 2000 observations for level and water flow rate and their corresponding residuals for the dissolution tank system. The training data containing two kinds of variation in the system: normal process variation and variation due to abnormality and noise. As can be seen in this figure, in the case of raw data there are many fluctuations in data and sometimes they exceed the threshold but in reality these were normal operational changes in the process. However this is not the issue in residuals as the residuals do not contain process variations. In case of level, 644 samples exceeded the threshold but in the corresponding residuals only 91 samples exceeded the threshold. Also in case of water flow rate, 782 samples exceeded the threshold but in the corresponding residuals only 114 samples exceeded the threshold which is reasonable because the selected PCs for this system shows 0.85 of variation in the system. Considering one standard deviation around the mean as normal threshold, the probability of level of the tank being in normal state is 71% for original data and is 93% for residuals. Also the probability of water flow rate being in normal state is 68% for original data and is 81% for residuals. This is because in original data some process normal variations are incorrectly considered as fault. So conditional probability values calculated from the residuals are more accurate than that of from raw data.



(a)



(b)

Figure 4.6. Process value and generated residuals of dissolution tank system. (a) Level (b) water flow rate

4.2.4. Loop handling

Since BN is acyclic network, while applying it for chemical processes with feedback controller or recycles, a special treatment is required to convert the network form cyclic to acyclic form. In order to capture the feedback effect in an acyclic network, we designed a duplicate dummy point as the feedback effect in recycle or controller. For example, in Fig. 4.7a, there is a causal relationship from X_i to X_o . Also based on the recycle loop there is a causal relationship from X_o to X_i as well. This loop has been treated as Fig. 4.7b and a dummy variable has been dedicated to variable X_i . It is obvious in Fig. 4.7b variable X_i has effect to variable X_o in the continuous line and also variable X_o has effect to variable X_i in the dash line.

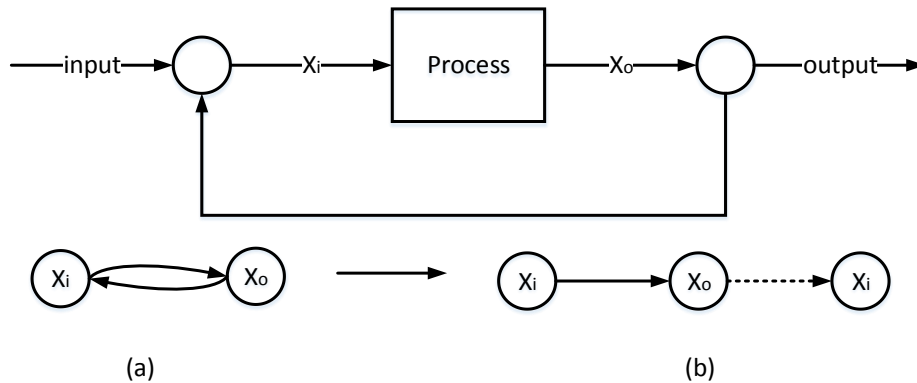


Figure 4.7. Loop handling in Bayesian network

4.3. Application of proposed methodology

In order to demonstrate the effectiveness of the proposed hybrid technique based on KPCA and BN, the methodology was applied to two case studies, one without recycle (FCC) and one with recycle (Tennessee Eastman):

Table 4.3. Measured variable of FCC process

No.	symbol	Variable
1	T_{air}	Air temperature
2	P_{si}	Coking factor
3	T_1	Fresh feed entering furnace
4	P_4	Reactor pressure
5	DP	Differential pressure
6	F_{air}	Air flow rate to regenerator
7	P_6	Regenerator pressure
8	T_3	Furnace temperature
9	T_2	Fresh feed entering to riser
10	T_r	Riser temperature
11	T_{reg}	Regenerator temperature
12	T_{cyc}	Cyclone temperature
13	C_{sc}	Coke frac. In spent catalyst
14	C_{rgc}	Coke frac. In regenerated catalyst

Table 4.4. Fault scenarios in FCC

Scenario No.	Fault description
1	5°C in atmosphere temperature
2	Gradual increase of 10°C in fresh feed temperature

Fault scenarios:

Step disturbance in ambient temperature: The first faulty scenario begins with normal operation for 1000 seconds and then is followed by a 5°C increase in ambient air temperature for the remaining 4000 seconds. The sampling time of the data generation is 1 second. The first 1000 fault free samples were used as training data. Gaussian function was selected as kernel function for KPCA. All data are normalized around zero. Five principal components were selected that explain 85% of the variations in the system. The value of threshold was calculated as 9.71 at 95% of confidence level. The Hotelling's T^2 and contribution plots of the KPCA analysis are shown in the Fig. 4.9. Based on Fig. 4.9a the Hotelling's T^2 identified departure from process normal condition. This plot depicts a successful detection of the abnormal condition. As can be seen, there is a long delay associated with the detection of this disturbance. It is because the magnitude of the variation in ambient temperature is not big enough to affect the process in a short time. Once the fault is detected, next step is to diagnose its root cause. The plot in Fig. 4.9c depicts the contribution plots to the T^2 . As it is obvious in Fig. 4.9c, when there is a disturbance in ambient temperature, the contribution plot cannot exactly diagnose the root cause of the fault, rather point towards few variables involved in the fault. However, regenerator pressure has the most contribution in this abnormal event, i.e. this variable has the highest variation among the variables in the propagation pathway of the fault.

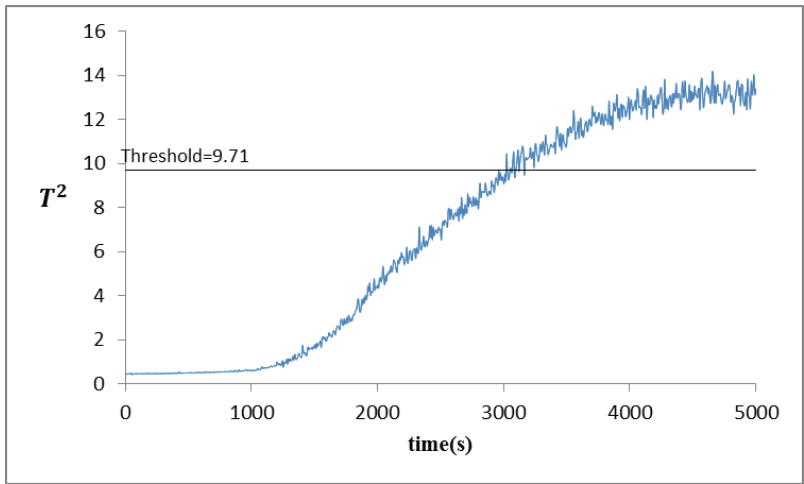


Fig 4.9 (a) Hotelling T^2 plot for disturbance in ambient air temperature in FCC

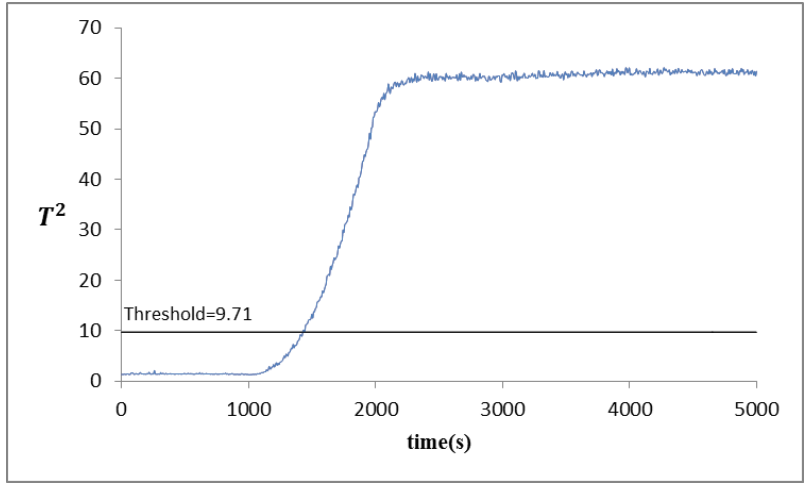


Fig 4.9 (b) Hotelling T^2 plot for disturbance in feed temperature in FCC

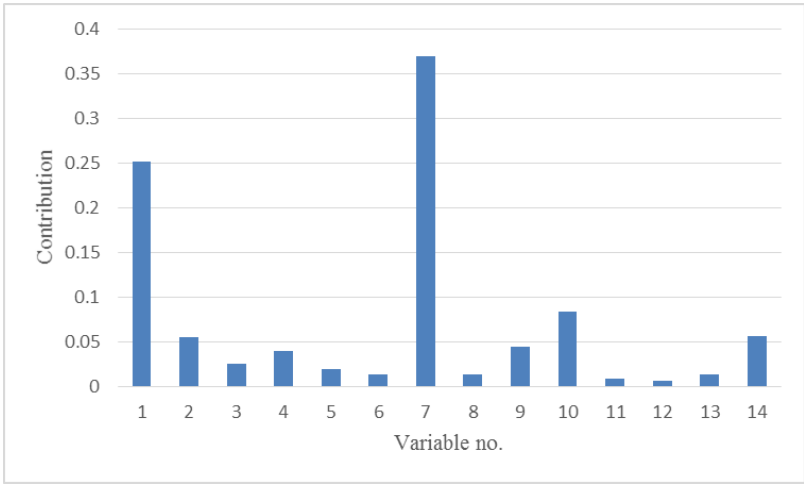


Fig 4.9 (c) Contribution plot for disturbance in ambient air temperature in FCC

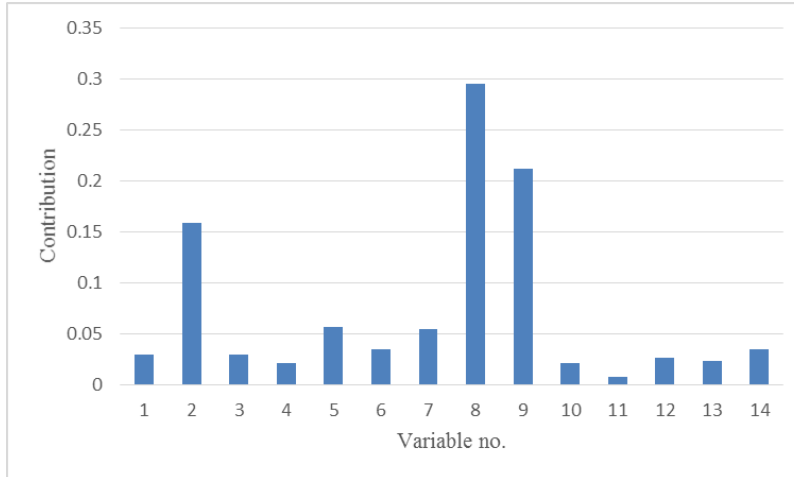


Fig 4.9 (d) Contribution plot for disturbance in feed temperature in FCC

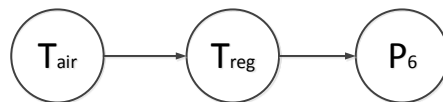
Having detected the fault, the first task is to determine whether this is a sensor fault or not. After testing all probable sensor faults, it was found that all sensors are working properly. Next we use BN to diagnose the root cause. In order to construct the network, all monitored variables and disturbances were considered as nodes. The cause and effect relationship between variables is determined by both causality analysis and process knowledge. Granger causality and transfer entropy were used to investigate the cause and effect relationship between variables and process knowledge that includes process flow diagram and expert knowledge were used as a confirmation to the constructed network. The conditional probabilities were obtained from historical data using MLE. In the historical data, both process faults were simulated (Table 4.4) and the data in training set are samples of all possible abnormal events. As explained in Section 4.2.4 the normal variation of process introduces inaccuracy in calculation of conditional probabilities. Therefore, the residuals of KPCA were used for conditional probability estimation.

When there is a variation in ambient temperature, based on the contribution plot (Fig. 4.9c), the regenerator pressure (P_6) has the highest variation among all monitored variables in the process. We take this variable as evidence [$P_{evidence\ node7} (state\ 0)=100\%$] for BN updating and for further analysis in BN to find out the propagation path and the true root cause of the fault. The updating

of the network was done using GeNIe software. The updated network for the faulty condition is shown in Fig. 4.10a. The state 0 shows the faulty state for each variable and state 1 shows the normal state. Based on this figure ambient air temperature has a probability of 88% to be in faulty state [$P_{T_{air}}(state=0)=88\%$], pointing this node as the most potential root cause of the fault and this variation propagated in this system through regenerator temperature and will be reflected in regenerator pressure. The propagation path is given in Fig. 4.10b.



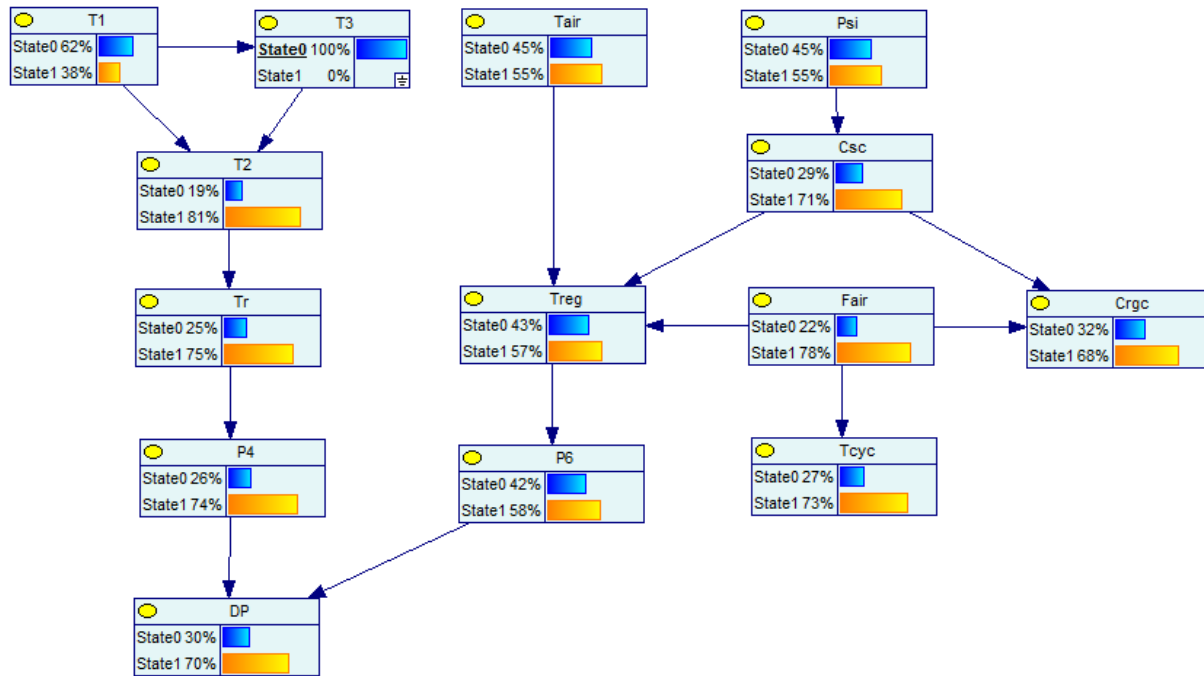
(a)



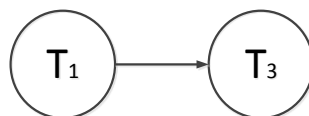
(b)

Figure 4.10. (a) BN for FCC process and (b) fault propagation pathway in FCC process for fault in ambient air temperature

Ramp disturbance on feed temperature: The second faulty scenario begins with normal operation for 1000 seconds and then is followed by a 10°C ramp in fresh feed temperature for the remaining 4000 seconds. The KPCA model construction is same as the first abnormal event. Fig. 4.9b shows the departure of T^2 values beyond the threshold that shows the successful detection of fault. After testing all sensors and being confident about their function, the root cause of the fault should be diagnosed among the internal states of the process. In the corresponding contribution plot (Fig. 4.9d) the furnace temperature has the highest contribution that means after the fault initiated this variable has the highest value of variation due to abnormality in the process. Based on this methodology this variable will be used as evidence node in the BN [$P_{evidence\ node8}(state\ 0)=100\%$]. Based on Fig. 4.11a, the updated network shows that the fresh feed temperature is the root cause of the abnormality in the process [$P_{T1}(state=0)=62\%$]. The propagation path is not lengthy and contains just two nodes (Fig. 4.11b).



(a)



(b)

Figure 4.11. (a) BN for FCC process and (b) fault propagation pathway in FCC process for fault in fresh feed temperature

4.3.2. Tennessee Eastman Chemical Process

In order to further illustrate the applicability of proposed method, the methodology is applied to benchmark Tennessee Eastman chemical process. The process consists of five major units: a reactor, condenser, compressor, separator, and stripper; and, it contains eight streams: A, B, C, D, E, F, G, and H. The flow diagram of this process is shown in Fig. 4.12. It consists of 41 measured variables and 12 manipulated variables. Among measured variables, 22 variables are continuous process variables and 19 variables are related to composition measurements. The 22 continuous

process variables are shown in Table 4.5 that are the main focus of this research. There are 20 potential faults in this process, among them we concentrate our study on those that are mentioned in Table 4.6 [3].

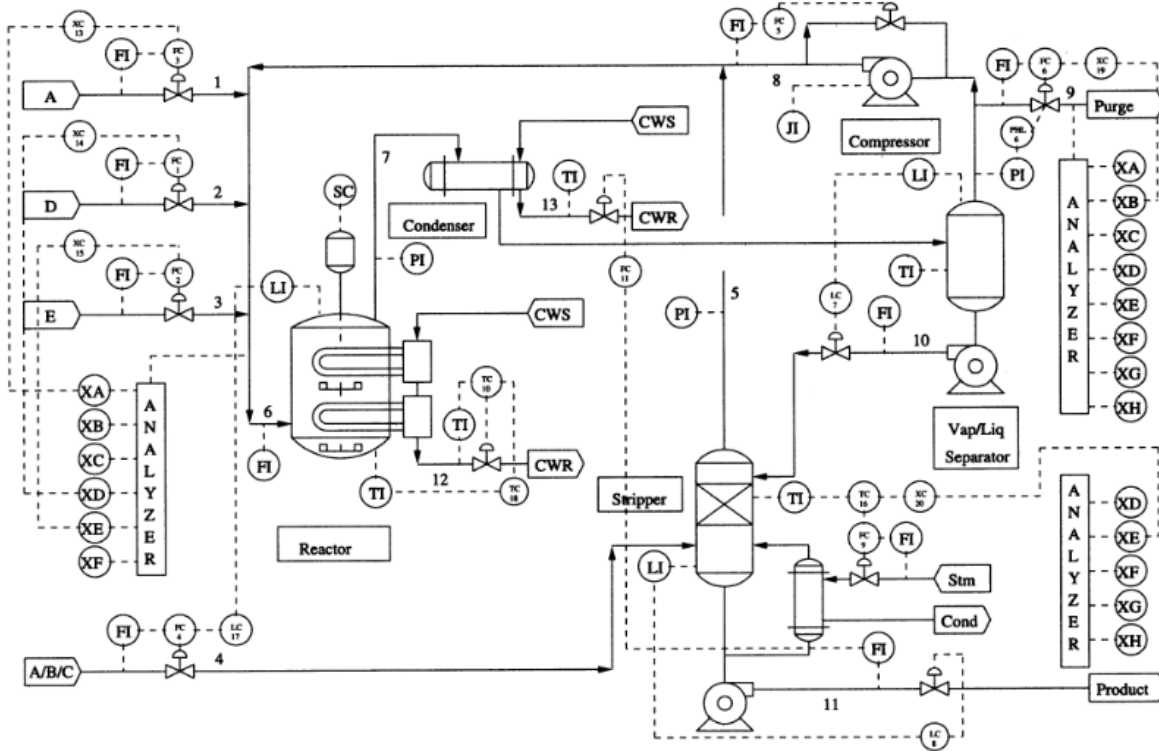


Figure 4.12. Schematic diagram of Tennessee Eastman process

Table 4.5. Measured variables in Tennessee Eastman

Variable	Description
XMEAS(1)	A Feed (stream 1)
XMEAS(2)	D Feed (Stream2)
XMEAS(3)	E Feed (Stream 3)
XMEAS(4)	Total Feed (Stream 4)
XMEAS(5)	Recycle Flow (Stream 8)
XMEAS(6)	Reactor Feed Rate (Stream6)
XMEAS(7)	Reactor Pressure
XMEAS(8)	Reactor Level
XMEAS(9)	Reactor Temperature
XMEAS(10)	Purge Rate (Stream 9)
XMEAS(11)	Separator temperature
XMEAS(12)	Separator level
XMEAS(13)	Separator pressure
XMEAS(14)	Separator Underflow (Stream 10)
XMEAS(15)	Stripper Level
XMEAS(16)	Stripper Pressure
XMEAS(17)	Stripper Underflow (Stream 11)
XMEAS(18)	Stripper Temperature
XMEAS(19)	Stripper Steam Flow
XMEAS(20)	Compressor Work
XMEAS(21)	Reactor Cooling Water Outlet temperature
XMEAS(22)	Separator Cooling Water Outlet Temperature

Table 4.6. Fault scenarios in Tennessee Eastman Chemical Process

Fault no.	Fault description
IDV(6)	Sudden loss of flow in feed A
IDV(12)	Random variation in condenser cooling water inlet temperature

Fault scenarios:

Sudden loss of feed A: The first faulty scenario is a loss in feed A at 500 second. This variation will affect the concentration of all components in the reactor. Consequently, this may change the process parameters in reactor and downstream units. A training set consisting of 500 samples from the normal data was used to develop the KPCA model. Gaussian kernel function was selected for linearization of data in KPCA. Four principal components were selected that captures 85% variation of the internal state of the process. The Hotelling’s T^2 statistic was equal to 21.5 at 95% of confidence level. Fig. 4.13a shows that KPCA is able to detect this fault due to exceeding of T^2 values beyond the threshold. After a delay of 20 seconds, there is a sharp jump in Hotelling’s T^2 values for this fault and these values exceed the threshold instantaneously when the abnormality initiated indicating that KPCA is able to detect the A feed loss quickly. Next we confirmed using the sensor check module that all sensors are functioning well and moved on to detect the propagation pathway of fault in internal states using BN.

The network construction and parameter estimation for Tennessee Eastman process was similar to FCC process using Granger causality and transfer entropy and was verified by process knowledge. Unlike FCC process, Tennessee Eastman contains a loop that makes the updating of the network

difficult. In order to deal with this issue, we designed a duplicate dummy point (pseudo point) for one of the variables involved in the loop. The constructed network in Fig. 4.14a shows that recycle flow, XMEAS(5), is involved in a loop in the network and was duplicated. One of these nodes is functioning as a parent node and the parameter estimation for this node was conducted like a parent node. The other node is like a child node and conditional probability values were considered for this node. Based on process knowledge it is obvious that variation in the feed A will affect the reactor feed rate because the inlet to the reactor is summation of A, D and E feeds. Since these feeds are gaseous, any variation in feed rate will affect the pressure in the reactor. Also it will affect the conversion due to change in residence time in the reactor which affects the temperature of the reactor due to the exothermic nature of the reaction. The contribution plot of each variable for the fault scenario is given in Fig. 4.13c. XMEAS(1), XMEAS(7), XMEAS(9) and XMEAS(21) have a high contribution in this faulty event; however, XMEAS(21) which is the reactor cooling water outlet temperature has the highest contribution and will be used as evidence in Bayesian network-based fault diagnosing module [$P_{XMEAS(21)} (state\ 0) = 100\%$]. The result of updated network is shown in Fig. 4.14a. As can be seen in this figure, a variation in the Feed A propagates through the network, affecting all nodes in propagation pathway, and eventually show up on XMEAS(21), as the last node in the propagation pathway. The probability of Feed A to be in faulty state is 78%. In this abnormal scenario, between the true root cause, XMEAS(1), and the faulty monitored variable, XMEAS(21), there are three intermediate variables (Fig. 4.14b).

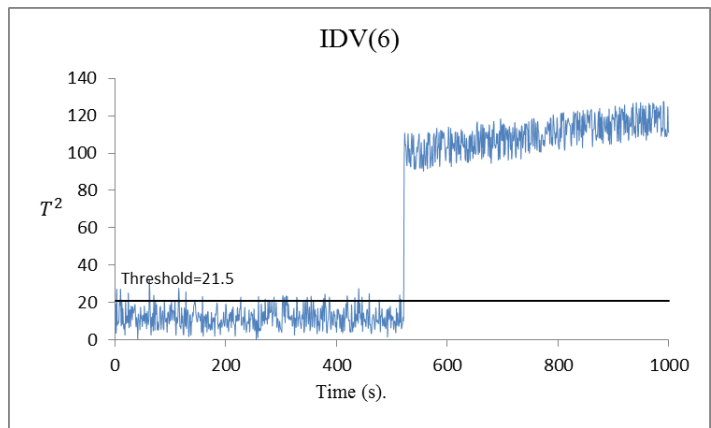


Fig 4.13 (a) Hotelling's T^2 for the fault IDV(6) in Tennessee Eastman process

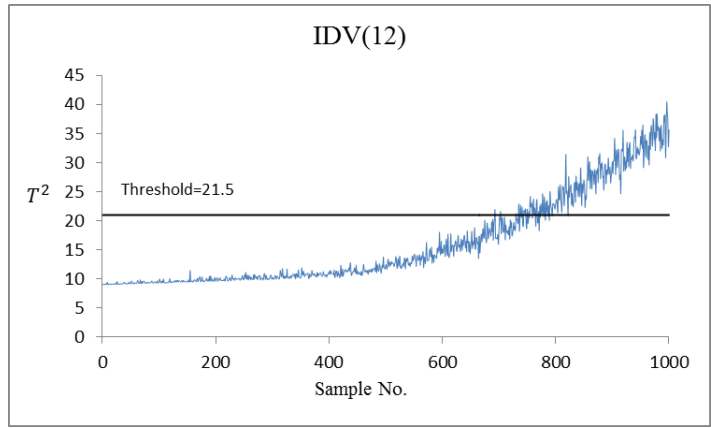


Fig 4.13 (b) Hotelling's T^2 for the fault IDV(12) in Tennessee Eastman process

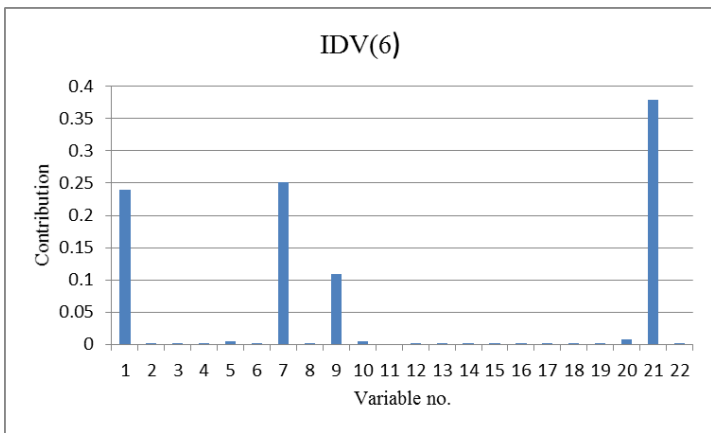


Fig 4.13 (c) Contribution plot for the fault IDV(6) in Tennessee Eastman process

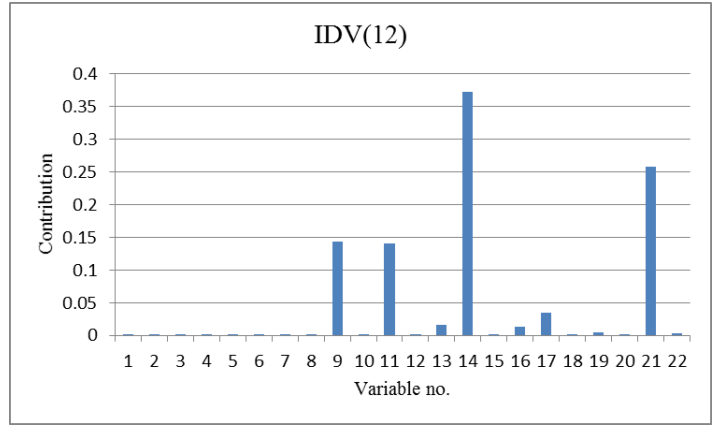
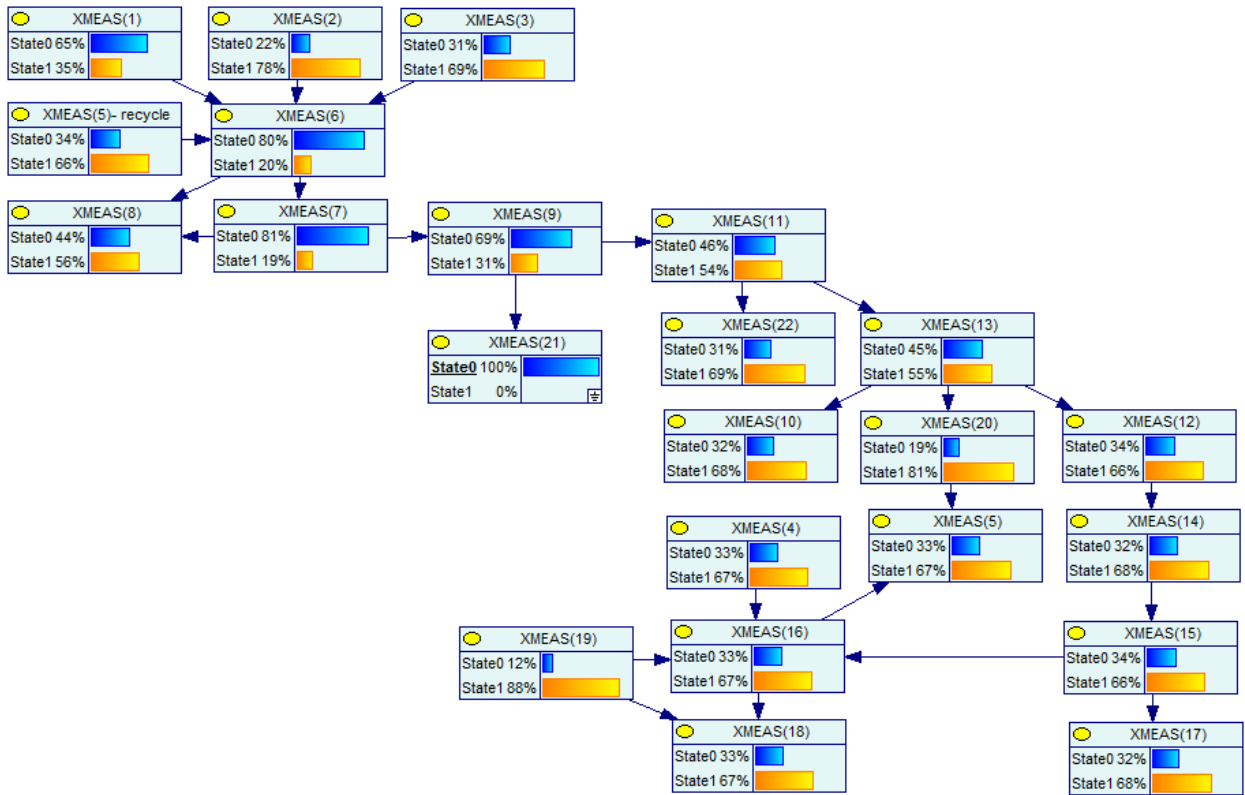
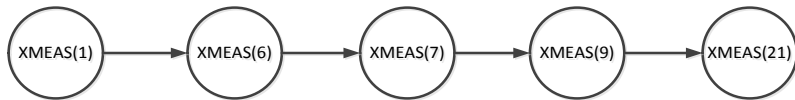


Fig 4.13 (d) Contribution plot for the fault IDV(12) in Tennessee Eastman process



(a)

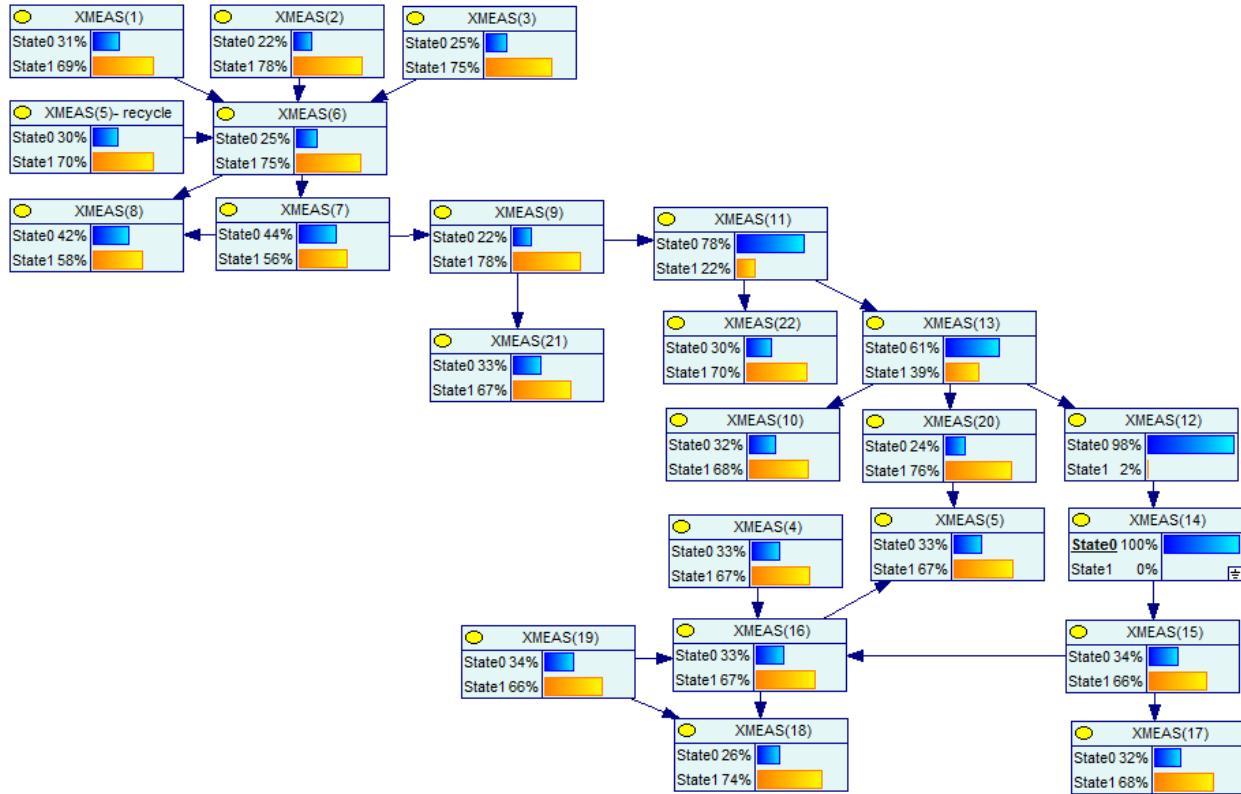


(b)

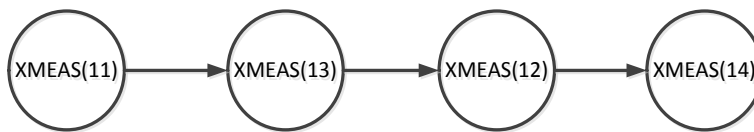
Figure 4.14. (a) BN for Tennessee Eastman and (b) fault propagation pathway for the fault IDV(6)

Fault in condenser cooling water inlet temperature: The fault initiated with a random variation in condenser cooling water inlet temperature at 500 seconds. This variable is not among measured variables. The source variables connected to this fault are in literatures [89]. Since the training data for both faulty scenarios in Tennessee Eastman are the same, the KPCA model for the second faulty scenario is the same as the first one. Fig. 4.13b shows the departure of T^2 values beyond the threshold (threshold=21.5). The random variation fault in the process variable was detected with a delay because the condenser cooling water inlet temperature is further downstream in the process and has less impact on the system compared to inlet feed.

In this abnormal event, XMEAS(9), XMEAS(11), XMEAS(14) and XMEAS(21) have the most contribution to occurrence of the fault(Fig. 4.13d); however, XMEAS(14), which is separator underflow, has the highest contribution and this node was considered as evidence node in the BN [$P_{XMEAS(14)}(state\ 0) = 100\%$]. The updated network shows that separator temperature, XMEAS(11), is the root cause of this abnormality, having a value of 0.78 as the probability for faulty state (Fig. 4.15a). In this abnormal event, a variation on the condenser cooling water inlet temperature will deviate away the temperature of the downstream unit (separator temperature or XMEAS(11)). Since there is no measurement in condenser cooling water inlet temperature, this method is able to find the variable that is mostly affected by the main root (XMEAS(11)) and is able to propagate the fault to other variables. As can be seen in Fig. 4.15b, this deviation will propagate through the network and will influence separator pressure, XMEAS(13), separator level, XMEAS(12), and eventually will effect separator underflow, XMEAS(14).



(a)



(b)

Figure 4.15. (a) BN for Tennessee Eastman and (b) fault propagation pathway for the fault IDV(12)

4.4. Conclusions

This paper integrates diagnostic information from different diagnostic tools (KPCA, sensor validation module) and combine them with process knowledge using BN and generates a comprehensive methodology for process FDD. We focused on the different challenges that have received less research focus such as network construction, conditional probability estimation, and

loop handling. Sensor faults were separated from process fault using a sensor check module. BN was used to diagnose internal state faults and disturbance faults. The proposed methodology was applied to test different abnormal condition of FCC and Tennessee Eastman Chemical process. In both case studies, the proposed methodology demonstrated a very powerful diagnostic capability. The strength of the proposed method is it diagnoses root cause of fault as well as shows the propagation pathway of the fault. This information will help operators to take corrective action and recover the process quickly. However, there is still more need for research in this area. For example, most of processes are working in dynamic condition and process variables change with time. In such problems conditional probability of a variable at time $t+1$ depends on its status at time t and dynamic BN should be implemented for such a problem to handle the dynamic relation of the variables.

Appendix -Kernel PCA calculations [87, 88]:

Given a sample containing n variables and m measurements, consider the nonlinear training set

$\mathbf{X} = [x_1 x_2 \dots x_m]^T$. An important property of the feature space is that the dot product of two vectors ϕ_i and ϕ_j can be calculated as a function of the corresponding vectors x_i and x_j , that is,

$$\phi_i^T \phi_j = k(x_i, x_j) \quad (1)$$

Assume that the vectors in the feature space are scaled to zero mean and form the training data as

$\chi = [\phi_1 \phi_2 \dots \phi_m]^T$. Let the sample covariance matrix of the data set in the feature space be S .

We have,

$$(m - 1)S = \chi^T \chi = \sum_{i=1}^m \phi_i \phi_i^T \quad (2)$$

Thus, KPCA in the feature space is equivalent to solving the following eigenvector equation,

$$\chi^T \chi v = \sum_{i=1}^m \phi_i \phi_i^T v = \lambda v \quad (3)$$

Kernel trick premultiplies Eq.3 by χ :

$$\chi \chi^T \chi v = \lambda \chi v \quad (4)$$

Defining

$$\mathbf{K} = \chi \chi^T = \begin{bmatrix} \phi_1^T \phi_1 & \dots & \phi_1^T \phi_m \\ \vdots & \ddots & \vdots \\ \phi_m^T \phi_1 & \dots & \phi_m^T \phi_m \end{bmatrix} = \begin{bmatrix} k(x_1, x_1) & \dots & k(x_1, x_m) \\ \vdots & \ddots & \vdots \\ k(x_m, x_1) & \dots & k(x_m, x_m) \end{bmatrix} \quad (5)$$

and denoting

$$\alpha = \chi v \quad (6)$$

we have

$$\mathbf{K} \alpha = \lambda \alpha \quad (7)$$

Equation 7 shows that α and λ are an eigenvector and eigenvalue of \mathbf{K} , respectively. In order to

solve v from Eq.6, we premultiply it by χ^T and use Eq.3,

$$\chi^T \boldsymbol{\alpha} = \chi^T \chi \boldsymbol{v} = \lambda \boldsymbol{v} \quad (8)$$

which shows that \boldsymbol{v} is given by

$$\boldsymbol{v} = \lambda^{-1} \chi^T \boldsymbol{\alpha} \quad (9)$$

Therefore, to calculate the PCA model, we first perform eigen-decomposition of Eq.7 to obtain λ_i and α_i . Then we use Eq.8 to find v_i .

Considering l principal components, the scores are calculated as:

$$\boldsymbol{t} = \boldsymbol{\Lambda}^{-1/2} \boldsymbol{P}^T \boldsymbol{k}(x) \quad (10)$$

where $\boldsymbol{P} = [\alpha_1^o \quad \dots \quad \alpha_l^o]$ and $\boldsymbol{\Lambda} = \text{diag}\{\lambda_1 \quad \dots \quad \lambda_l\}$ are the l principal eigenvector and eigenvalues of \mathbf{K} and $\alpha_i = \sqrt{\lambda_i} \alpha_i^o$ and $\boldsymbol{k}(x)$ is:

$$\begin{aligned} \boldsymbol{k}(x) = \chi \boldsymbol{\phi} &= [\phi_1 \quad \phi_2 \quad \dots \quad \phi_m]^T \boldsymbol{\phi} = [\phi_1^T \boldsymbol{\phi} \quad \phi_2^T \boldsymbol{\phi} \quad \dots \quad \phi_m^T \boldsymbol{\phi}] = \\ &[k(x_1, x) \quad k(x_2, x) \quad \dots \quad k(x_m, x)]^T \end{aligned} \quad (11)$$

The T^2 is calculated using kernel function as

$$T^2 = \boldsymbol{k}(x)^T \boldsymbol{P} \boldsymbol{\Lambda}^{-2} \boldsymbol{P}^T \boldsymbol{k}(x) = \boldsymbol{k}(x)^T \boldsymbol{D} \boldsymbol{k}(x) \quad (12)$$

$$\text{where } \boldsymbol{D} = \boldsymbol{P} \boldsymbol{\Lambda}^{-2} \boldsymbol{P}^T \quad (13)$$

Scaling:

The calculation of covariance matrix holds if the mapping function in the feature space has zero mean. If this not the case, the vectors in the feature space have to be scaled to zero mean using the sample mean of the training data. The scaling of the kernel vector $\boldsymbol{k}(x)$ is

$$\bar{\boldsymbol{k}}(x) = [\bar{\phi}_1 \quad \bar{\phi}_2 \quad \dots \quad \bar{\phi}_m]^T \bar{\boldsymbol{\phi}} = \boldsymbol{F}[\boldsymbol{k}(x) - \boldsymbol{K} \mathbf{1}_m] \quad (14)$$

Where $\boldsymbol{F} = \boldsymbol{I} - \boldsymbol{E}$, \boldsymbol{I} is the identity matrix, \boldsymbol{E} is an $m \times m$ matrix with elements $1/m$ and $\mathbf{1}_m$ is a m dimensional vector whose elements are $1/m$.

Reconstruction-based contribution of variable:

The procedure to estimate fault free data by applying a correction in the faulty data is referred to as reconstruction. Reconstruction of the fault free data from faulty measurements can be done by estimating the fault magnitude along the fault direction. The task of fault reconstruction is to estimate the normal values z_i , by eliminating the effect of a fault f_i from faulty data x_i ,

$$z_i = x_i - \xi_i f_i \quad (15)$$

where ξ_i is the fault direction. The objective of reconstructed based contribution is to find the magnitude f_i of a vector with direction such ξ_i that the fault detection Index of the reconstructed measurement is minimized; that is, we want to find f_i such that

$$f_i = \arg \min \text{Index}(x - \xi_i f_i) \quad (16)$$

The same concept can be applied to KPCA and find f_i such that

$$f_i = \arg \min \text{Index}(\mathbf{k}(x - \xi_i f_i)) \quad (17)$$

The T^2 Index is as follows:

$$\text{index} = \bar{\mathbf{k}}(z_i)^T D \bar{\mathbf{k}}(z_i) \quad (18)$$

$\bar{\mathbf{k}}(z_i)$ is scaled kernel vector. The derivative of the Index with respect to f_i is

$$\frac{\partial(\text{index})}{\partial(f_i)} = 2 \bar{\mathbf{k}}^T(z_i) D \frac{\partial \bar{\mathbf{k}}(z_i)}{\partial f_i} \quad (19)$$

The scaled kernel vector is $\bar{\mathbf{k}}(z_i) = \mathbf{F}[\mathbf{k}(z_i) - \mathbf{K} \mathbf{1}_m]$. Then, we have that

$$\frac{\partial \bar{\mathbf{k}}(z_i)}{\partial f_i} = \mathbf{F} \frac{\partial \mathbf{k}(z_i)}{\partial f_i} \quad (20)$$

So the derivative of Index will be

$$\frac{\partial(\text{Index})}{\partial(f_i)} = 2 F D \bar{\mathbf{k}}^T(z_i) \frac{\partial \mathbf{k}(z_i)}{\partial f_i} \quad (21)$$

To calculate the derivative of $\mathbf{k}(z_i)$ with respect to f_i , we now that

$$\frac{\partial \mathbf{k}(z_i)}{\partial f_i} = \frac{\partial \mathbf{k}(z_i)}{\partial z_i} \frac{\partial z_i}{\partial f_i} \quad (22)$$

Since $\mathbf{k}(z_i) = [k(z_i, x_1), k(z_i, x_2) \dots k(z_i, x_m)]$ and $k(z_i, x_j) = \exp(-(z_i - x_j)^T (z_i - x_j)/c)$,

we have

$$\frac{\partial}{\partial z_i} k(z_i, x_j) = -2k(z_i, x_j) \frac{(z_i - x_j)^T}{c} \quad (23)$$

and

$$\frac{\partial z_i}{\partial z_i} = -\xi_i \quad (24)$$

Therefore, the vector with the derivative of $\mathbf{k}(z_i)$ respect to f_i

$$\frac{\partial \mathbf{k}(z_i)}{\partial f_i} = \frac{2}{c} \begin{bmatrix} k(z_i, x_1)(z_i - x_1)^T \\ k(z_i, x_1)(z_i - x_2)^T \\ \vdots \\ k(z_i, x_m)(z_i - x_m)^T \end{bmatrix} \xi_i = \frac{2}{c} \begin{bmatrix} k(z_i, x_1)(x - x_1)^T - k(z_i, x_1)f_i \xi_i^T \\ k(z_i, x_1)(x - x_2)^T - k(z_i, x_2)f_i \xi_i^T \\ \vdots \\ k(z_i, x_m)(x - x_m)^T - k(z_i, x_m)f_i \xi_i^T \end{bmatrix} = \frac{2}{c} [\mathbf{B}\xi_i - \mathbf{k}(z_i)f_i] \quad (25)$$

Where \mathbf{B} is calculated as

$$\mathbf{B} = \begin{bmatrix} k(z_i, x_1)(x - x_1)^T \\ k(z_i, x_1)(x - x_2)^T \\ \vdots \\ k(z_i, x_m)(x - x_m)^T \end{bmatrix} \quad (26)$$

We can now calculate the derivative of Index as

$$\frac{\partial(\text{index})}{\partial f_i} = \frac{4}{c} FD\bar{\mathbf{K}}^T(z_i)[\mathbf{B}\xi_i - \mathbf{k}(z_i)f_i] \quad (27)$$

After setting the derivative equal to zero and solving for f_i we obtain

$$f_i = \frac{\xi_i^T \mathbf{B}^T FD\bar{\mathbf{k}}(z_i)}{\bar{\mathbf{k}}^T(z_i) FD\bar{\mathbf{k}}(z_i)} \quad (28)$$

Chapter 5

Summary conclusion and future work

In this thesis, the problem of collecting different fault diagnostic information and integrating them in a complete framework for early detection of a process abnormality and diagnosing the root cause of the failure is investigated. This thesis proposed two frameworks based on causality analysis and BN as strong tools for diagnosing root cause of fault. Also there are some ambiguity in the application of Bayesian network for example, validating the causal relationships between variables, estimation of parameters of network, dealing with cyclic network, and distinguishing between instrumental failure and process failure which are addressed in this thesis.

5.1. Conclusions

- While applying different diagnostic tools, the outputs of some diagnostic tools contain useful information for other tools. In other words integrating some diagnostic methods and using their information in a hybrid framework will increase the accuracy of fault diagnosis task.
- The sensitivity of KPCA to process variation is a promising point in the detection of an abnormality in the process. Although sometimes its detection is delayed depending of the magnitude of the abnormality, but even after a considerable lag it can detect the occurrence

of the abnormality quite early. Additionally the delay can be adjusted with the KPCA parameters such as confidence level and number of PCs.

- KPCA method is not a strong tool in diagnosis and in the contribution plots it delivers some of the variables which has a substantial variations after the abnormality initiated. The root cause is often between the isolated variables indicating that the variation of the root cause of the abnormality leads to variation in the other nodes which are located in the propagation pathway.
- Granger causality and transfer entropy can determine the causal relation between variables and are useful tools for network construction, but in case of having few variables they can be used to recognize the root cause in qualitative manner.
- Although TE and Granger causality have different definitions but for variables with normal distributions they provide the same results.
- Process variation is mitigated in residuals which are obtained from process data, however they keep the information of the data; resulting in more precise network parameter estimation.

5.2. Suggestions for future work

- Chemical processes operate in dynamic mode; resulting in time series data, and the status of a variable is determined based on its past status and the effect of other variables. In such a problems, using Dynamic Bayesian Network will contribute to more precise diagnostic.
- Process recovery is the next step of fault detection and diagnosis methodology in which an action should be taken in order to mitigate the effect of the fault in whole process and keep the process in safe mode. This research did not work in this area; however it is worthwhile to integrate fault diagnostic method with process recovery.

- In sensor fault detection module, we kept the methodology simple by using rule based sensor fault detection module; however, bank of Kalman filters which is more precise method will result in a better sensor fault detection module and can be integrated with this methodology.

References:

1. Dong, J., et al., *Adaptive total PLS based quality-relevant process monitoring with application to the Tennessee Eastman process*. Neurocomputing, 2015. **154**: p. 77-85.
2. Murray, R.M., et al., *Future directions in control in an information-rich world*. IEEE Control Systems Magazine, 2003. **23**(2): p. 20-33.
3. Chiang, L.H., R.D. Braatz, and E.L. Russell, *Fault detection and diagnosis in industrial systems*. 2001: Springer Science & Business Media.
4. Venkatasubramanian, V., et al., *A review of process fault detection and diagnosis: Part III: Process history based methods*. Computers & chemical engineering, 2003. **27**(3): p. 327-346.
5. Chen, J.Z.B. and J. Shen, *A hybrid ANN-ES system for dynamic fault diagnosis of hydrocracking process*. Computers & chemical engineering, 1997. **21**: p. S929-S933.
6. Mylaraswamy, D. and V. Venkatasubramanian, *A hybrid framework for large scale process fault diagnosis*. Computers & chemical engineering, 1997. **21**: p. S935-S940.
7. Psychogios, D.C. and L.H. Ungar, *A hybrid neural network-first principles approach to process modeling*. AIChE Journal, 1992. **38**(10): p. 1499-1511.
8. Isermann, R., *Model-based fault-detection and diagnosis—status and applications*. Annual Reviews in control, 2005. **29**(1): p. 71-85.
9. Hu, J., et al., *An integrated safety prognosis model for complex system based on dynamic Bayesian network and ant colony algorithm*. Expert Systems with Applications, 2011. **38**(3): p. 1431-1446.
10. Venkatasubramanian, V., R. Rengaswamy, and S.N. Kavuri, *A review of process fault detection and diagnosis: Part II: Qualitative models and search strategies*. Computers & Chemical Engineering, 2003. **27**(3): p. 313-326.
11. Ma, J. and J. Jiang, *Applications of fault detection and diagnosis methods in nuclear power plants: A review*. Progress in nuclear energy, 2011. **53**(3): p. 255-266.
12. Frank, P.M. and X. Ding, *Survey of robust residual generation and evaluation methods in observer-based fault detection systems*. Journal of process control, 1997. **7**(6): p. 403-424.
13. Isermann, R., *Process fault detection based on modeling and estimation methods—a survey*. Automatica, 1984. **20**(4): p. 387-404.
14. Willsky, A.S., *A survey of design methods for failure detection in dynamic systems*. Automatica, 1976. **12**(6): p. 601-611.
15. Gertler, J.J., *Survey of model-based failure detection and isolation in complex plants*. Control Systems Magazine, IEEE, 1988. **8**(6): p. 3-11.
16. Frank, P.M., *Fault diagnosis in dynamic systems using analytical and knowledge-based redundancy: A survey and some new results*. Automatica, 1990. **26**(3): p. 459-474.
17. Basseville, M., *Detecting changes in signals and systems—a survey*. Automatica, 1988. **24**(3): p. 309-326.
18. Frank, P.M. and B. Köppen-Seliger, *New developments using AI in fault diagnosis*. Engineering Applications of Artificial Intelligence, 1997. **10**(1): p. 3-14.
19. Garcia, E.A. and P. Frank, *Deterministic nonlinear observer-based approaches to fault diagnosis: a survey*. Control Engineering Practice, 1997. **5**(5): p. 663-670.
20. Frank, P., S. Ding, and T. Marcu, *Model-based fault diagnosis in technical processes*. Transactions of the Institute of Measurement and Control, 2000. **22**(1): p. 57-101.
21. Chow, E.Y. and A.S. Willsky, *Analytical redundancy and the design of robust failure detection systems*. Automatic Control, IEEE Transactions on, 1984. **29**(7): p. 603-614.
22. Gertler, J. and D. Singer, *A new structural framework for parity equation-based failure detection and isolation*. Automatica, 1990. **26**(2): p. 381-388.

23. Venkatasubramanian, V., et al., *A review of process fault detection and diagnosis: Part I: Quantitative model-based methods*. Computers & chemical engineering, 2003. **27**(3): p. 293-311.
24. Cho, J.-H., et al., *Fault identification for process monitoring using kernel principal component analysis*. Chemical engineering science, 2005. **60**(1): p. 279-288.
25. Webb, A.R., *Statistical pattern recognition*. 2003: John Wiley & Sons.
26. Jackson, J.E., *A user's guide to principal components*. Vol. 587. 2005: John Wiley & Sons.
27. Hastie, T., *Principal curves and surfaces*. 1984, DTIC Document.
28. Schölkopf, B. and A.J. Smola, *Learning with kernels: Support vector machines, regularization, optimization, and beyond*. 2002: MIT press.
29. Tipping, M.E. and C.M. Bishop, *Mixtures of probabilistic principal component analyzers*. Neural computation, 1999. **11**(2): p. 443-482.
30. Zhao, S.J. and Y.M. Xu. *Levenberg-Marquardt algorithm for nonlinear principal component analysis neural network through inputs training*. in *Intelligent Control and Automation, 2004. WCICA 2004. Fifth World Congress on*. 2004. IEEE.
31. Lawrence, N., *Probabilistic non-linear principal component analysis with Gaussian process latent variable models*. The Journal of Machine Learning Research, 2005. **6**: p. 1783-1816.
32. Ham, J., et al. *A kernel view of the dimensionality reduction of manifolds*. in *Proceedings of the twenty-first international conference on Machine learning*. 2004. ACM.
33. Harkat, M.F., G. Mourot, and J. Ragot. *Nonlinear PCA combining principal curves and RBF-networks for process monitoring*. in *Decision and Control, 2003. Proceedings. 42nd IEEE Conference on*. 2003. IEEE.
34. Mallick, M.R. and S. Imtiaz. *A Hybrid Method for Process Fault Detection and Diagnosis*. in *Dynamics and Control of Process Systems*. 2013.
35. Dunia, R., et al., *Identification of faulty sensors using principal component analysis*. AIChE Journal, 1996. **42**(10): p. 2797-2812.
36. Yu, H., F. Khan, and V. Garaniya, *Modified Independent Component Analysis and Bayesian Network-Based Two-Stage Fault Diagnosis of Process Operations*. Industrial & Engineering Chemistry Research, 2015. **54**(10): p. 2724-2742.
37. Fussell, J., E. Henry, and N. Marshall, *MOCUS: A computer program to obtain minimal sets from fault trees*. 1974, Aerojet Nuclear Co., Idaho Falls, Idaho (USA).
38. Hessian Jr, R.T., B.B. Salter, and E.F. Goodwin, *Fault-tree analysis for system design, development, modification, and verification*. Reliability, IEEE Transactions on, 1990. **39**(1): p. 87-91.
39. Shiozaki, J. and F. Miyasaka. *A fault diagnosis tool for HVAC systems using qualitative reasoning algorithms*. in *Proceedings of the Building Simulation*. 1999.
40. Maurya, M.R., R. Rengaswamy, and V. Venkatasubramanian, *A systematic framework for the development and analysis of signed digraphs for chemical processes. 1. Algorithms and analysis*. Industrial & Engineering Chemistry Research, 2003. **42**(20): p. 4789-4810.
41. Wang, X., et al., *Qualitative process modelling-a fuzzy signed directed graph method*. Computers & chemical engineering, 1995. **19**: p. 735-740.
42. Lee, E., Y. Park, and J.G. Shin, *Large engineering project risk management using a Bayesian belief network*. Expert Systems with Applications, 2009. **36**(3): p. 5880-5887.
43. Heckerman, D., *Bayesian networks for data mining*. Data mining and knowledge discovery, 1997. **1**(1): p. 79-119.
44. Heckerman, D., A. Mamdani, and M.P. Wellman, *Real-world applications of Bayesian networks*. Communications of the ACM, 1995. **38**(3): p. 24-26.
45. Fan, C.-F. and Y.-C. Yu, *BBN-based software project risk management*. Journal of Systems and Software, 2004. **73**(2): p. 193-203.

46. Ülengin, F., et al., *An integrated transportation decision support system for transportation policy decisions: The case of Turkey*. Transportation Research Part A: Policy and Practice, 2007. **41**(1): p. 80-97.
47. Uusitalo, L., *Advantages and challenges of Bayesian networks in environmental modelling*. Ecological modelling, 2007. **203**(3): p. 312-318.
48. Van Der Gaag, L.C., *Bayesian belief networks: odds and ends*. The Computer Journal, 1996. **39**(2): p. 97-113.
49. Zhao, Y., F. Xiao, and S. Wang, *An intelligent chiller fault detection and diagnosis methodology using Bayesian belief network*. Energy and Buildings, 2013. **57**: p. 278-288.
50. Azhdari, M. and N. Mehranbod. *Application of Bayesian belief networks to fault detection and diagnosis of industrial processes*. in *Chemistry and Chemical Engineering (ICCCE), 2010 International Conference on*. 2010. IEEE.
51. Lauritzen, S.L. and F. Jensen, *Stable local computation with conditional Gaussian distributions*. Statistics and Computing, 2001. **11**(2): p. 191-203.
52. Madsen, A.L., *Belief update in CLG Bayesian networks with lazy propagation*. International Journal of Approximate Reasoning, 2008. **49**(2): p. 503-521.
53. Verron, S., J. Li, and T. Tiplica, *Fault detection and isolation of faults in a multivariate process with Bayesian network*. Journal of Process Control, 2010. **20**(8): p. 902-911.
54. Krishnamoorthy, G., P. Ashok, and D. Tesar, *Simultaneous Sensor and Process Fault Detection and Isolation in Multiple-Input-Multiple-Output Systems*. 2014.
55. Mehranbod, N., et al., *Probabilistic model for sensor fault detection and identification*. AIChE Journal, 2003. **49**(7): p. 1787-1802.
56. Dey, S. and J. Stori, *A Bayesian network approach to root cause diagnosis of process variations*. International Journal of Machine Tools and Manufacture, 2005. **45**(1): p. 75-91.
57. Yu, J. and M.M. Rashid, *A novel dynamic bayesian network-based networked process monitoring approach for fault detection, propagation identification, and root cause diagnosis*. AIChE Journal, 2013. **59**(7): p. 2348-2365.
58. Alessandri, A., *Fault diagnosis for nonlinear systems using a bank of neural estimators*. Computers in industry, 2003. **52**(3): p. 271-289.
59. Zhang, X., M.M. Polycarpou, and T. Parisini, *A robust detection and isolation scheme for abrupt and incipient faults in nonlinear systems*. Automatic Control, IEEE Transactions on, 2002. **47**(4): p. 576-593.
60. Sobhani-Tehrani, E., H.A. Talebi, and K. Khorasani, *Hybrid fault diagnosis of nonlinear systems using neural parameter estimators*. Neural Networks, 2014. **50**: p. 12-32.
61. Ren, Z., et al. *A combined method based on neural network for control system fault detection and diagnosis*. in *Control Applications, 2000. Proceedings of the 2000 IEEE International Conference on*. 2000. IEEE.
62. Ferdowsi, H., *Model based fault diagnosis and prognosis of nonlinear systems*. 2013.
63. Venkatasubramanian, V. and S. Rich, *An object-oriented two-tier architecture for integrating compiled and deep-level knowledge for process diagnosis*. Computers & Chemical Engineering, 1988. **12**(9): p. 903-921.
64. Becraft, W.R., P.L. Lee, and R.B. Newell. *Integration of Neural Networks and Expert Systems for Process Fault Diagnosis*. in *IJCAI*. 1991. Citeseer.
65. Himes, D.M., R.H. Storer, and C. Georgakis. *Determination of the number of principal components for disturbance detection and isolation*. in *American Control Conference, 1994*. 1994. IEEE.
66. Schwartz, G., *Estimating the order of a model*. The Annals of Statistics, 1978. **2**: p. 461-464.
67. Barnett, L. and A.K. Seth, *The MVGC multivariate Granger causality toolbox: a new approach to Granger-causal inference*. Journal of neuroscience methods, 2014. **223**: p. 50-68.

68. Yang, F., L.S. Sirish, and D. Xiao. *Signed directed graph modeling of industrial processes and their validation by data-based methods*. in *Control and Fault-Tolerant Systems (SysTol), 2010 Conference on*. 2010. IEEE.
69. Granger, C.W., *Investigating causal relations by econometric models and cross-spectral methods*. *Econometrica: Journal of the Econometric Society*, 1969: p. 424-438.
70. Feige, E.L. and D.K. Pearce, *The casual causal relationship between money and income: Some caveats for time series analysis*. *The Review of Economics and Statistics*, 1979: p. 521-533.
71. Duan, P., et al., *A New Information Theory-Based Method for Causality Analysis*. 2014.
72. Schreiber, T., *Measuring information transfer*. *Physical review letters*, 2000. **85**(2): p. 461.
73. Bauer, M., et al., *Finding the direction of disturbance propagation in a chemical process using transfer entropy*. *Control Systems Technology, IEEE Transactions on*, 2007. **15**(1): p. 12-21.
74. Vicente, R., et al., *Transfer entropy—a model-free measure of effective connectivity for the neurosciences*. *Journal of computational neuroscience*, 2011. **30**(1): p. 45-67.
75. Barnett, L., A.B. Barrett, and A.K. Seth, *Granger causality and transfer entropy are equivalent for Gaussian variables*. *Physical review letters*, 2009. **103**(23): p. 238701.
76. Hlaváčková-Schindler, K., *Equivalence of Granger causality and transfer entropy: a generalization*. *Applied Mathematical Sciences*, 2011. **5**(73): p. 3637-3648.
77. Hiemstra, C. and J.D. Jones, *Testing for linear and nonlinear Granger causality in the stock price-volume relation*. *The Journal of Finance*, 1994. **49**(5): p. 1639-1664.
78. Diks, C. and V. Panchenko, *A new statistic and practical guidelines for nonparametric Granger causality testing*. *Journal of Economic Dynamics and Control*, 2006. **30**(9): p. 1647-1669.
79. Parente, A., et al., *Identification of low-dimensional manifolds in turbulent flames*. *Proceedings of the Combustion Institute*, 2009. **32**(1): p. 1579-1586.
80. Boser, B.E., I.M. Guyon, and V.N. Vapnik. *A training algorithm for optimal margin classifiers*. in *Proceedings of the fifth annual workshop on Computational learning theory*. 1992. ACM.
81. Wiener, N., *The theory of prediction*. *Modern mathematics for engineers*, 1956. **1**: p. 125-139.
82. Akaike, H., *A new look at the statistical model identification*. *Automatic Control, IEEE Transactions on*, 1974. **19**(6): p. 716-723.
83. Schwartz, G., *Estimating dimension or" a model*. *Arm Star*. 1978161461464.. Fedomk MN. GimenezABonufe P.(ions ES, Mayer LD. Nelson CC. P-glycoprotein increases the ethnic of the androgen dihydmtosterone and reduces androgen responsive gene activity in prostate tumor cells. *Pmsrore. ZW: 59: 77—90*. Lu, 1978.
84. Liu, L. and J. Wan, *The relationships between Shanghai stock market and CNY/USD exchange rate: New evidence based on cross-correlation analysis, structural cointegration and nonlinear causality test*. *Physica A: Statistical Mechanics and its Applications*, 2012. **391**(23): p. 6051-6059.
85. Silverman, B.W., *Density estimation for statistics and data analysis*. Vol. 26. 1986: CRC press.
86. McFarlane, R.C., et al., *Dynamic simulator for a model IV fluid catalytic cracking unit*. *Computers & chemical engineering*, 1993. **17**(3): p. 275-300.
87. Alcalá, C.F. and S.J. Qin, *Reconstruction-based contribution for process monitoring with kernel principal component analysis*. *Industrial & Engineering Chemistry Research*, 2010. **49**(17): p. 7849-7857.
88. Qin, S.J., *Survey on data-driven industrial process monitoring and diagnosis*. *Annual Reviews in Control*, 2012. **36**(2): p. 220-234.
89. Chang, J.L., *A Fault Diagnosis Based On Fault Magnitude Strategy For Tennessee Eastman Process*. 2013.
90. Zhou, Y., *Data driven process monitoring based on neural networks and classification trees*. 2005, Texas A&M University.

91. Willsky, A.S. and H.L. Jones. *A generalized likelihood ratio approach to state estimation in linear systems subjects to abrupt changes*. in *Decision and Control including the 13th Symposium on Adaptive Processes, 1974 IEEE Conference on*. 1974. IEEE.
92. Kresta, J.V., J.F. MacGregor, and T.E. Marlin, *Multivariate statistical monitoring of process operating performance*. *The Canadian Journal of Chemical Engineering*, 1991. **69**(1): p. 35-47.
93. Li, W. and S. Shah, *Structured residual vector-based approach to sensor fault detection and isolation*. *Journal of Process Control*, 2002. **12**(3): p. 429-443.
94. Kobayashi, T. and D.L. Simon. *Evaluation of an enhanced bank of Kalman filters for in-flight aircraft engine sensor fault diagnostics*. in *ASME Turbo Expo 2004: Power for Land, Sea, and Air*. 2004. American Society of Mechanical Engineers.
95. Sharma, A.B., L. Golubchik, and R. Govindan, *Sensor faults: Detection methods and prevalence in real-world datasets*. *ACM Transactions on Sensor Networks (TOSN)*, 2010. **6**(3): p. 23.
96. Duan, P., et al., *Direct causality detection via the transfer entropy approach*. *Control Systems Technology, IEEE Transactions on*, 2013. **21**(6): p. 2052-2066.
97. Yang, F., et al., *Capturing connectivity and causality in complex industrial processes*. 2014: Springer Science & Business Media.